SPECIAL REINFORCED MASONRY SHEAR WALL FUNCTIONAL RECOVERY PREQUALIFICATION

Final Report Submitted to the PUC (1/5/2026) for Consideration in the 2026 NEHRP Provisions

FUNCTIONAL RECOVERY PREQUALIFICATION REPORT FOR SPECIAL REINFORCED MASONRY SHEAR WALLS

Final Report Submitted to the PUC for Consideration in the 2026 NEHRP Provisions

Prepared By:

Resilient Design Coalition

Financially Supported by:

Concrete Masonry & Hardscapes Association, Concrete Masonry Checkoff, and the Charles Pankow Foundation

TECHNICAL WORK AND AUTHORSHIP BY:

Ed Almeter, MS
Kristen Blowes, PhD, PE
Jared DeBock, PhD, PE
Curt Haselton, PhD, PE
Carlos Molina Hutt, PhD, PE
Huy Pham, PhD
David Welch, PhD
Reid Zimmerman, SE

January 5, 2026

QUANTIFICATION OF FUNCTIONAL RECOVERY SEISMIC PERFORMANCE FACTORS FOR SPECIAL REINFORCED MASONRY SHEAR WALLS

Submitted: 1/5/2026

EXECUTIVE SUMMARY

A quantification of the functional recovery seismic performance factors for the Special Reinforced Masonry Shear Wall (SRMSW) lateral force resisting system is performed in accordance with the proposed Section A.8.3.6 procedures in Appendix A of the 2026 National Earthquake Hazards Reduction Program (NEHRP) Provisions. The assessments documented herein cover the design of buildings with SRMSW lateral force-resisting systems in accordance with Chapter 12 of ASCE 7-22. Design coefficients and factors for life-safety design are based on the bearing wall configuration of line A.8 of Table 12.2-1 in ASCE 7-22, "special reinforced masonry shear walls." The response modification factor, R, is 5, the overstrength factor, Ω, is 2.5, and the deflection amplification factor, C_d, is 3.5. All designs investigated herein satisfy the life-safety design provisions of ASCE 7-22.

Appendix A of the 2026 NEHRP Provisions provides additional design requirements to satisfy functional recovery performance objectives at the Functional Recovery Earthquake (FRE_R) level shaking. The functional recovery seismic performance factors include the functional recovery response modification coefficient, R_{fr}, functional recovery allowable story drift limit, Δ_{afr}, and the functional recovery structure ductility reduction factor, $R_{\mu fr}$. Drift checks are performed with C_d equal to R_{fr} for functional recovery design.

R_{fr} and Δ_{afr} were determined by developing an archetype space of different building heights, designed with various functional recovery response modification coefficients and allowable drift limits, and then selecting the combination that results in less than a 10% mean probability of Safety-Critical Structural Damage, or P[SCSD], in each performance group, and less than 20% P[SCSD] for any individual archetype, for Functional Recovery Category (FRC) A, B and C. The 10% and 20% thresholds are modified to 15% and 25%, respectively, for FRC D. All analyses are conducted at the Functional Recovery Earthquake (FRE_R) level shaking corresponding to a Seismic Design Category $D_{max,FRE}$ condition with two-point spectral ordinates S_{dsfr} and S_{d1fr} of 1.25g and 0.75g, respectively. The required values of R_{fr} and Δ_{afr} derived from analysis are compared with the judgment-based limits in Appendix A of NEHRP 2026, and the more stringent values are selected. The judgment-based limits of R_{fr} are R/1.5 and R/1.25 for FRC A/B/C and FRC D, respectively. The judgment-based limit, Δ_{afr}, is set at 1% for all FR categories, since the life-safety drift limit for SRMSW is a constant 1% regardless of Risk Category. System-specific $R_{\mu fr}$ factors are determined by comparing peak floor acceleration demands from the analysis with the seismic floor accelerations from Section A.10.6 in accordance with Section A.8.3.6 procedures in Appendix A of the 2026 NEHRP Provisions.

The proposed R_{fr}, Δ_{afr}, and $R_{\mu fr}$ for the SRMSW lateral force-resisting system from the qualification assessment are presented in Table 1 for flexure-controlled walls (SRMSW-F) and in Table 2 for walls containing shear-controlled wall piers (SRMSW-S).

Results from the assessment showed that the functional recovery performance factors for shear-controlled SRMSWs were primarily governed by damage in the masonry shear wall in the mid-rise performance group, with the resulting design requirements governed by the max acceptance criteria. Flexure-controlled SRMSWs were governed by damage in the masonry shear walls in both performance groups, with the resulting design requirements governed by the mean criteria. For shear-controlled SRMSWs, a R_{fr} of 2.5 and 3.0 achieves the performance goals for FRC A/B/C and FRC D, respectively, at the design drift limit Δ_{afr} of 0.5%. For flexure-controlled SRMSW, R_{fr} values of 3.5 and 4.0 achieve the performance goals for FRC A/B/C and FRC D, respectively, at the design drift limit Δ_{afr} of 0.50%.

Table 1. Summary of functional recovery seismic performance factors for SRMSW-F lateral systems.

	FRC A/B/C			**FRC D**		
	R_{fr}	**Δ_{afr}**	**$R_{\mu fr}$†**	**R_{fr}**	**Δ_{afr}**	**$R_{\mu fr}$†**
Analysis results	3.5	0.5%	0.85	4.0	0.5%	0.90
Judgment-based upper limit	3.5	1.0%	--	4.0	1.0%	--
Recommendation – SRMSW-F	**3.5**	**0.5%**	**0.85**	**4.0**	**0.5%**	**0.90**

†$R_{\mu fr}$ is only calculated for the recommended seismic performance factors

Table 2. Summary of functional recovery seismic performance factors for SRMSW-S lateral systems.

	FRC A/B/C			**FRC D**		
	R_{fr}	**Δ_{afr}**	**$R_{\mu fr}$†**	**R_{fr}**	**Δ_{afr}**	**$R_{\mu fr}$†**
Analysis results	2.5	0.5%	0.65	3.0	0.5%	0.70
Judgment-based upper limit	3.5	1.0%	--	4.0	1.0%	--
Recommendation – SRMSW-S	**2.5**	**0.5%**	**0.65**	**3.0**	**0.5%**	**0.65**

†$R_{\mu fr}$ is only calculated for the recommended seismic performance factors

ContentsS

1. INTRODUCTION

This report documents the quantification of the functional recovery seismic performance factors for the special reinforced masonry shear wall (RMSW) system. Quantification of the functional recovery seismic performance factors is performed in accordance with the procedures proposed in Section A.8.3.6 of the 2026 National Earthquake Hazards Reduction Program (NEHRP) Provisions. The functional recovery seismic performance factors include the functional recovery response modification coefficient, R_{fr}, the functional recovery allowable story drift limit, Δ_{afr}, and the functional recovery structure ductility reduction factor, $R_{\mu fr}$. These are the equivalents of the response modification coefficient, R, the allowable story drift limit, Δ_a, and the structure ductility reduction factor, R_μ, used in ASCE/SEI 7 Chapters 12 and 13, but for design for functional recovery.

An archetype space of different building heights, designed with various functional recovery response modification coefficients and allowable drift limits, was developed. FEMA P-58/ATC-138 (FEMA, 2018a; ATC, 2021) models were then created. In accordance with the proposed Section A.8 procedures of the 2026 NEHRP Provisions, only structural components are included in these FEMA P-58/ATC-138 performance models. Design of the archetypes was performed using the automated design capability of SP3 (www.sp3risk.com). Engineering demand parameters (e.g., story drift ratios, peak floor accelerations, etc.) were estimated using SP3's Response Prediction Engine, which, while calibrated based on extensive nonlinear response history analyses, does not perform nonlinear response history analyses of the specific archetype directly.

Performance assessments of each model are conducted in accordance with FEMA P-58 (FEMA, 2018a) and ATC-138 recommendations to quantify the probability of safety-critical structural damage (P[SCSD]) for each archetype (Blowes et al., in press). The assigned safety class governs the triggering of SCSD for a given component and damage state according to the ATC-138 methodology. The safety class controls the maximum percentage of components in each story and direction that can be in each damage state or greater before triggering SCSD in the building. The P[SCSD] serves as an acceptable proxy for the probability of exceeding the target functional recovery times for structural-only models, as outlined in section CA.8.3.5 of the 2026 NEHRP Seismic Provisions.

The functional recovery seismic performance factors are selected such that archetypes designed for that R_{fr} and Δ_{afr} result in less than a 10% mean P[SCSD] in each performance group and less than 20% P[SCSD] for any individual archetype for Functional Recovery Category (FRC) A, B and C. The 10% and 20% thresholds are modified to 15% and 25%, respectively, for FRC D. These limits are in accordance with the proposed Section A.8.3.6 procedures of the 2026 NEHRP Provisions. All analyses are conducted at the Functional Recovery Earthquake (FRE_R) level shaking corresponding to a Seismic Design Category $D_{max,FRE}$ condition with two-point spectral ordinates S_{dsfr} and S_{d1fr} of 1.25g and 0.75g, respectively.

2. ANALYSIS METHODS

2.1. Design Iteration and Acceptance Criteria for Seismic Performance Factors

For each individual archetype, design iterations are carried out using values of R_{fr} and Δ_{afr} across the ranges of 1 through R (i.e., up to the response modification coefficient used in life-safety design) and 0.1% through 1.0% in increments of 0.1% (i.e., up to the maximum allowable story drift ratio), respectively. The Response Modification Factor, R, is 5 for SRMSW systems, in accordance with Table 12.2-1 of ASCE 7-22 (ASCE, 2022). These design iterations are performed using the SP3 design engine, which estimates the strength and stiffness of each design to obtain appropriate structural responses and subsequent estimates of SCSD.

In each performance group, the combination of R_{fr} and Δ_{afr} is deemed to be acceptable if the mean P[SCSD] is less than 10%, and the maximum P[SCSD] across all archetypes in the performance group is less than 20% for quantifying the functional recovery seismic performance factors for FRC A, B, and C. For FRC D, the mean and maximum P[SCSD] across all archetypes in a performance group must be less than 15% and 25%, respectively. The recommended design values for a particular system are taken as the most restrictive across all performance groups, rounded to the nearest increment considered (0.5 for R_{fr} and 0.1% for Δ_{afr}).

The requirements of the proposed Section A.8.3.6 procedures of the 2026 NEHRP Provisions impose that R_{fr} shall not be taken greater than R/1.5 for FRC A, B, and C, and R/1.25 for FRC D. The value of Δ_{afr} is not taken as greater than 1% for all FRCs in the SRMSW analysis, since the life-safety drift limit for SRMSW is a constant 1% regardless of Risk Category. Additionally, to verify the strength-stiffness coupling inherent to each design variant, each archetype model is reassessed under an independent strength-stiffness assumption, i.e., where additional strength prescribed by R_{fr} does not result in additional stiffness to the building. Analysis outcomes from the independent-strength-and-stiffness assessment are checked to ensure the maximum P[SCSD] does not exceed the acceptance criteria (20% for FRC A/B/C and 25% for FRC D), where applicable. The judgment-based upper limit and the independent-strength-and-stiffness check provide a reasonable limit, preventing excessive reliance on the analytical results and recognizing the historical precedent set by the higher Risk Categories.

2.1.1. Safety-Critical Structural Damage (SCSD)

The assigned safety class governs the triggering of SCSD for a given component and damage state according to the ATC-138 methodology (ATC, 2021). The safety class controls the percentage of components in each story and direction that can be in each damage state or greater before triggering SCSD. A summary of the ATC-138 safety class descriptions and acceptance thresholds is shown in Table 3.

Table 3. ATC-138 safety-class definitions for triggering SCSD (ATC, 2021).

Safety Class	Description	Acceptance Threshold[a]
0	Slight damage that is not a safety concern and will never trigger an unsafe placard	N/A
1	Moderate damage that may be visually concerning, but does not substantially reduce the lateral strength of the component.	50%
2	Severe damage that causes substantial loss of lateral strength of the component, but does not substantially reduce its vertical load-carrying capacity.	25%
3	Severe damage that compromises both the lateral and vertical load-carrying capacity of the component.	10%

[a] Percentages reflect the upper quantity of components, in each story and direction, that can be in a safety class of interest before triggering safety-critical structural damage (SCSD). The safety-critical structural damage check is performed independently for each system in the building (e.g., the gravity vs. lateral system).

2.2. Fragility Functions for SRMSWs

Fragility functions relate structural responses to the likelihood of damage and its consequences. Fragility functions are commonly modeled by a lognormal distribution defined by a lognormal mean (θ) and standard deviation (β). For a given structural component, sequential damage states (DSs) can be represented by individual fragility functions that describe the likelihood of a distinct level of damage, the corresponding repair effort, and the associated consequences. Additionally, damage states may be mutually exclusive, with a single fragility function representing multiple outcomes (i.e., sub-damage states). Each likelihood is assigned a weighting that sums to unity (e.g., 0.25 + 0.75 = 1). More general background information on fragility functions and damage state development can be found in FEMA P-58-1 (FEMA, 2018a).

The following sub-sections provide details on the structural component fragility functions, including:

- Special Reinforced Masonry Shear Walls
- Bolted shear tab gravity connections

Foundation elements are considered rugged in the current analysis. Fragility functions for foundation elements were not developed during the FEMA P-58 project, and foundation elements are included explicitly in the list of acceptable rugged components in Appendix I of FEMA P-58-1 (FEMA, 2018a).

2.2.1. Special Reinforced Masonry Shear Walls

Fragility functions for in-plane damage to special reinforced masonry shear walls were developed as part of the FEMA P-58 fragility database (FEMA, 2009b; Murcia-Delso and Shing, 2012). Fragilities for reinforced masonry shear walls are derived from a review of 69 wall specimen tests across eight experimental studies, mostly consisting of single-story, fully grouted, specially reinforced wall segments. Separate fragilities for reinforced masonry walls were developed for both special and ordinary reinforcing, for flexure- and shear-dominated behavior, and for fully and partially grouted walls.

Walls dominated by flexure can exhibit relatively ductile behavior, depending on the axial load and the longitudinal reinforcement. Larger axial compressive load and the flexural reinforcement ratio delay flexural yielding and result in less ductile walls. Damage in flexure-dominated walls typically begins with very minor diagonal cracking just after first yield (DS1). At peak strength, there is a noticeable but limited toe crushing identified by vertical cracks in the toe region or light toe spalling (DS2). Finally, the 20% strength loss coincides with out-of-plane buckling, severe toe crushing, or bar buckling and/or fracture (DS3), resulting in costly and complex repairs (i.e., demolition and replacement). For clarity, flexure-controlled fragilities exclusively interpreted DS1, DS2, and DS3 as the points corresponding to 80% pre-peak strength, peak strength, and 80% post-peak strength, respectively, to avoid subjectivity in data interpretation (FEMA, 2009b). An illustration of the typical damage progression in flexure-dominated, special reinforced masonry walls is shown in Figure 1. Additional examples of toe crushing at peak strength (DS2) are provided in Figure 2.

DS1 is attributed to Safety Class 0, since it represents cosmetic damage due to cracking. DS2 is assigned to Safety Class 1, which considers that peak strength has been reached in the specimen and the remaining post-peak ductility can be variable depending on numerous factors including: the amount of longitudinal reinforcement, level of axial load and presence of lap splices within the plastic hinge region (Sherman, 2011; Ahmadi, 2012; NIST, 2017). Notably, FEMA P-58 and ATC-138 did not associate DS2 with SCSD, yet this change is deemed appropriate based on review of recent testing of RM shear walls and the allowance of lap splices within the plastic hinge by the IBC (Kingsley et al. 2014). DS3 is assigned to Safety Class 3, representing significant strength loss in a vertical load bearing element.

By contrast, in shear-dominated masonry walls, behavior is often very brittle. Before the shear capacity of a wall has been reached, minor diagonal cracks may form (DS1), requiring epoxy injection. However, once the wall's peak strength is reached, the lateral resistance can drop rapidly, as evidenced by the formation of major diagonal cracks (DS2), resulting in costly and complex repairs (i.e., demolition and replacement). Similar to flexure-controlled walls, DS2 was directly interpreted as the deformation demand corresponding to peak strength. DS1 and DS2 for shear-dominated walls are assigned to Safety Class 0 and 3, respectively. An illustration of the typical damage progression in shear-dominated special reinforced masonry walls is shown in Figure 3. A summary of the SRMSW fragility functions and corresponding safety classes is provided in Table 4 and Table 5 for flexure-dominated and shear-dominated wall behavior, respectively. All SRMSW fragilities in this study use wall chord rotation as the primary EDP.

Damage State 1 | Damage State 2 | Damage State 3

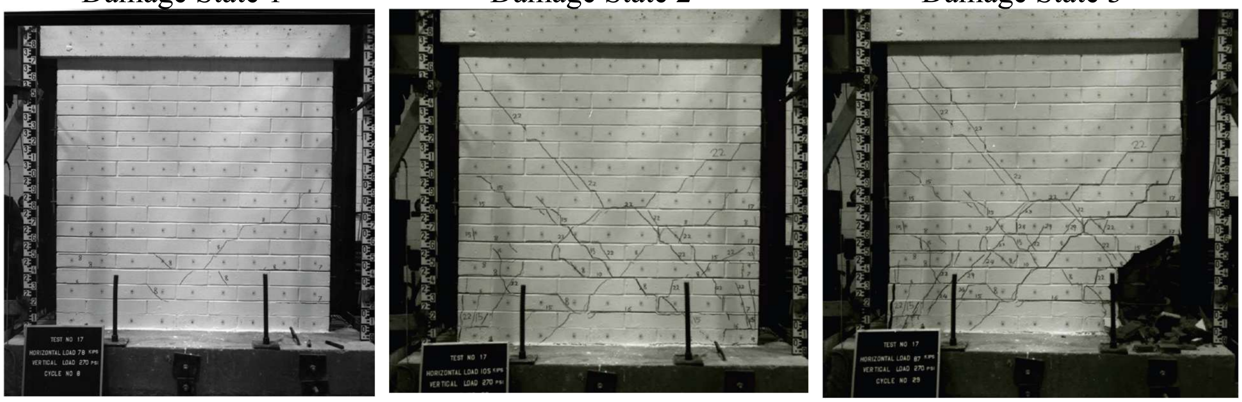

Figure 1 – Illustration of damage states for flexure-dominated special reinforced masonry walls. Images from the FEMA P-58 background document BD-3.8.10 (FEMA, 2009b). Testing conducted by Shing et al. (1991).

a) b) c)

Figure 2 – Examples of toe-crushing at peak strength associated with Damage State 2 for flexure-dominated walls: a, b) Sherman (2011) – Specimen 1A, 1B; c) Ahmadi (2012) – Specimen UT-W-13

Damage State 1 Damage State 2

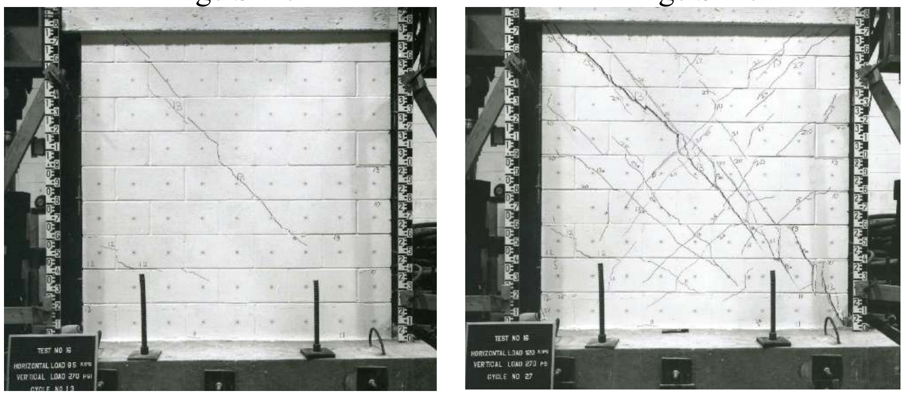

Figure 3 – Illustration of damage states for shear-dominated special reinforced masonry walls. Images from the FEMA P-58 background document BD-3.8.10 (FEMA, 2009b). Testing conducted by Shing et al. (1991).

Table 4 – FEMA P-58: Flexure-dominated special reinforced masonry walls, fragility damage states, and safety classes.

Damage State	**Median Chord Rotation (θ)[a]**	**β**	**Safety Class[b]**	**Damage Description**	**Repair Measures**
DS1	0.31%	0.47	0	A few flexural and shear cracks with hardly noticeable residual crack widths. Slight yielding of extreme vertical reinforcement. No spalling. No fracture or buckling of vertical reinforcement. No structurally significant damage.	Cosmetic repair. Patch cracks and paint each side.
DS2	0.9%	0.4	1[c]	Numerous flexural and diagonal cracks with residual crack widths less than 1/64 in. Mild toe crushing with vertical cracks or light spalling at wall toes. No fracture or buckling of reinforcement. Small residual deformation. Damage corresponds to reaching peak strength.	Epoxy injection to repair cracks. Remove loose masonry. Patch spalls with non-shrink grout. Paint each side.
DS3	1.51%	0.32	3	Severe flexural cracks with residual crack widths greater than 1/32 in. Severe toe crushing and spalling. Fracture or buckling of vertical reinforcement. Significant residual deformation. Damage corresponds to 20% post-peak strength.	Shore. Demolish existing wall. Construct new wall.

[a] Fragility function is a lognormal distribution with median and standard deviation of θ and β, respectively. The EDP is wall chord rotation.
[b] SC 1 = 50%, SC 2 = 25%, SC 3 = 10% allowable quantity of damaged component per direction per story; SC 0 cannot cause SCSD.
[c] This safety class definition deviates from the original FEMA P-58 and ATC-138 documentation.

Table 5 – FEMA P-58: Shear-dominated special reinforced masonry walls, fragility damage states, and safety classes.

Damage State	Median Chord Rotation (θ)[a]	β	Safety Class[b]	Damage Description	Repair Measures
DS1	0.36%	0.59	0	First occurrence of major diagonal cracks. Cracks remain closed with hardly noticeable residual crack widths after load removal.	Epoxy injection at cracks. Paint each side.
DS2	0.59%	0.51	3	Wide diagonal cracks with typically one or more cracks in each direction. Crushing or spalling at wall toes.	Shore. Demolish existing wall. Construct new wall.

[a] Fragility function is a lognormal distribution with median and standard deviation of θ and β, respectively. The EDP is wall chord rotation.
[b] SC 1 = 50%, SC 2 = 25%, SC 3 = 10% allowable quantity of damaged component per direction per story; SC 0 cannot cause SCSD.

In this study, we considered fully grouted special reinforced masonry walls in our quantification of functional recovery seismic performance factors, populating both flexure-dominated and shear-dominated wall segment fragilities into the archetype performance models as applicable.

TMS 402/602-16 (TMS, 2016) allows for both flexure-dominated and shear-dominated walls, provided they meet the shear capacity requirements of Section 7.3.2.6.1.1:

"7.3.2.6.1.1 When designing special reinforced masonry shear walls to resist in-plane forces in accordance with Section 9.3 [strength design]*, the design shear strength, φV_n, shall exceed the shear corresponding to the development of 1.25 times the nominal flexural strength, M_n, of the element, except that the nominal shear strength, V_n, need not exceed 2.5 times required shear strength, V_u."*

Flexure-dominated response is ensured through capacity designing the wall to have adequate shear strength to develop the flexural strength of the section. Conversely, when this is not possible, shear-controlled walls must provide adequate shear-strength to reliably withstand design forces by providing a minimum of 2.5 times the shear demand. This option sacrifices ductility for much higher strength in order to protect against brittle shear failure.

The original FEMA P-58 database reported the EDP as 'story drift ratio', but this is inconsistent with the experimental basis as well as the original intent of the developers of the fragility functions. From an experimental standpoint, all fully grouted tests used for fragility development were conducted with cantilever loading conditions, with the top of the wall free to rotate for both flexure- and shear-controlled walls. Although each experimental test was interpreted as top displacement over wall height (i.e., a drift ratio), this reflects displacement at the effective height of the wall (point of zero moment) and does not relate to individual story drift ratios in multistory buildings. Murcia-Delso and Shing (2012; FEMA, 2009b) caution users of the fragilities to consider that multi-story buildings should use a modified drift demand in upper stories according to $(\Delta/h)_{def} = \Delta/h - \theta$, where Δ/h represents the story drift at a given upper story and θ is the rigid body rotation from the base of the wall. This adjustment would avoid conservative demands being estimated in upper stories, yet could be unconservative for estimating total demands at the base of the wall based solely on story drift demand, since the 'experimental drift ratio' used for fragility development represents the total rotation at the effective height of the wall. Based on this, the use of wall chord rotation in terms of demand and capacity is assumed to be the most consistent. More discussion on the estimation of wall chord rotation demands is provided in Section 2.4.4. Additional details on the experimental testing and fragility development can be found in the FEMA P-58 background document BD-3.8.10 (FEMA, 2009b) and Murcia-Delso and Shing (2012).

2.2.2. Steel Gravity Connection Fragilities

Steel gravity beam-to-column connections are based on fragility development by Deierlein and Victorsson (2008) during the FEMA P-58 Project and are available within the FEMA P-58 fragility database. The fragilities are based on thirteen experimental tests on simple bolted shear tab connections conducted by Liu and Astaneh (2000). Fragilities are developed using story drift ratio as the EDP.

Fragility functions for steel gravity connections comprise three sequential damage states, with DS1 split into two mutually exclusive DSs: conduct or neglect minor repairs. DS2 is assigned a Safety Class of 2, while DS3 is assigned a Safety Class of 3. ATC-138 assigned Safety Class 2 to both DS2 and DS3. Following review of the damage description for DS3, the Safety Class was increased to 3 to better align with the Safety Class definitions (see Table 3), based on the peer review committee's judgment. A summary of the fragility functions and corresponding safety class assignments is provided in Table 6. Figure 4 shows example photographs of each damage state. A plot of the fragility functions is provided in Figure 5.

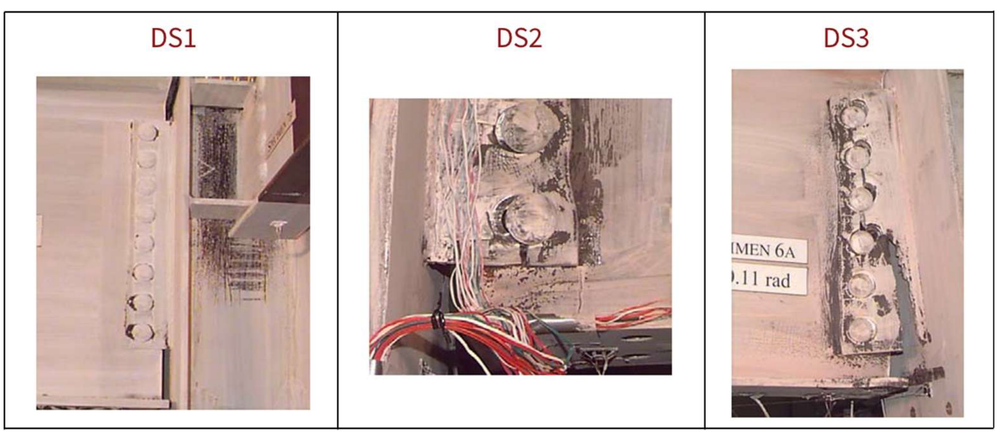

Figure 4 – Illustration of damage states for steel shear tab connections (Deierlein and Victorsson, 2008).

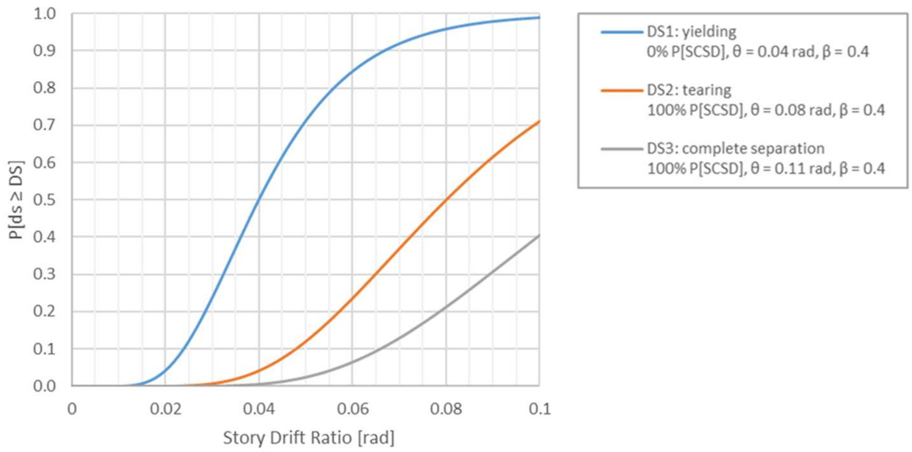

Figure 5 – Fragility functions for bolted shear tab gravity connections.

Table 6. Bolted shear tab gravity connection fragility damage states and corresponding safety classes.

Damage State[a]	**Median (θ)[b]**	**β**	**Safety Class[c]**	**Damage Description**	**Repair Measures**
DS1a (0.95)	4.00%	0.4	0	Yielding of shear tab and elongation of bolt holes, possible crack initiation around bolt holes or at shear tab weld. Damage in field is either obscured or deemed to not warrant repair. No repair conducted.	Careful inspection and welded repair to any cracks and possible replacement of shear tab if bolt hole deformations are excessive (possible for deeper 6-bolt or deeper shear tabs). Field condition is deemed to not warrant repair by field observation.
DS1b (0.05)	4.00%	0.4	0	Yielding of shear tab and elongation of bolt holes, possible crack initiation around bolt holes or at shear tab weld.	Careful inspection and welded repair to any cracks and possible replacement of shear tab if bolt hole deformations are excessive (possible for 6-bolt or deeper shear tabs).
DS2	8.00%	0.4	2	Partial tearing of shear tab and possibility of bolt shear failure (6-bolt or deeper connections).	Repairs will include either welded repair of shear tab or possible complete replacement of shear tab and installation of new bolts. Repairs may require shoring of beam.
DS3	11.00%	0.4	3[d]	Complete separation of shear tab, close to complete loss of vertical load resistance.	Repair will include complete replacement of shear tab and installation of new bolts. Repairs will require shoring of beam.

[a] Mutually exclusive damage states (e.g., DSXa and DSXb) include the probability of occurrence in parentheses
[b] Fragility function is a lognormal distribution with median and standard deviation of θ and β, respectively. The EDP is story drift ratio.
[c] SC 1 = 50%, SC 2 = 25%, SC 3 = 10% allowable quantity of damaged components per direction per story; SC 0 does not result in SCSD.
[d] This assessment deviates from the ATC 138 assignment of DS3 as Safety Class 2 based on a review of the safety class definitions and the judgment of the authors and peer review team.

2.3. Archetypes Considered for Analysis

To determine the combination of R_{fr} and Δ_{afr} that results in acceptable functional recovery performance, an archetype space is divided into performance groups, analyzed, and the overall parameters are determined from the worst-case performance group. This is similar to the FEMA P-695 methodology used to quantify life-safety performance factors (FEMA, 2009) and is in accordance with the proposed Section A.8 procedures of the 2026 NEHRP Provisions.

2.3.1. Building Configuration and Structural Component Population

All archetypes assume a constant plan area of 140 feet by 70 feet and an 11-foot story height. There are two primary variants considered for the SRMSW archetype: The number of stories and the presence of shear-controlled wall segments. Building heights range from 2 to 12 stories, split into two height classes: low-rise (2, 3, and 4 stories) and mid-rise (6, 8, 10, and 12 stories). Reinforced masonry shear walls are arranged around the perimeter of the structure, concentrated in the corners of the building, with light-frame cladding panels between them. Typical plan layouts and populated structural components are shown in Figure 6. Structural bays are arranged on a 14-foot grid, with steel gravity columns at each grid point. Steel shear tab gravity connections are assumed at all locations outside the SRMSW.

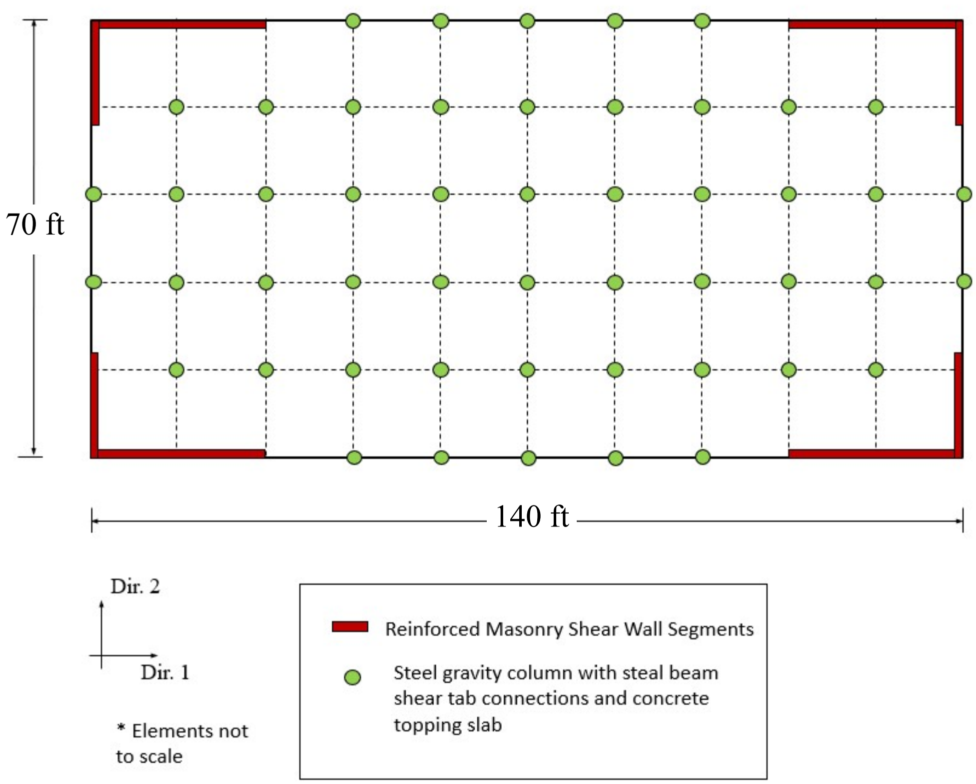

Figure 6 – Illustration of assumed plan layouts for SRMSW archetypes with population of structural components.

2.3.2. *Performance Groups for SRMSW*

Performance groups are delineated based on building characteristics that influence the structural properties and global response of SRMSW buildings. The performance group heights considered were low-rise (PG1) and mid-rise (PG2) SRMSW buildings. The use of building height to define (or delineate) performance groups has strong precedence in numerous applications of the FEMA P-695 methodology, which serves as the basis for the performance group concept used in the current study and for the underlying NEHRP Appendix A provisions. As a minimum, performance groups are distinguished between short-period (short structures) and long-period (tall structures).

Within the low-rise and mid-rise performance groups, two archetype variants are assessed: buildings with and without shear-controlled wall segments. For variants with shear-controlled wall segments, the ratio of shear-controlled segments to total wall segments ranges from 5% (primarily flexural walls) to 100% (all shear-controlled walls). This variation in ratio causes variation in two key aspects of the analysis. The first has to do with the 10% damage threshold for SC3 (the SC of DS2 of shear-controlled walls); when adding in the more sensitive shear-controlled walls, it becomes much more likely at lower drifts that this threshold will be exceeded once the ratio of shear-controlled walls exceeds 10% of the total number of walls. The second aspect is the extra design requirements for shear-controlled walls imposed by TMS 402-16 Section 7.3.2.6.1.1 that significantly increases the overstrength of those walls as described in Section 2.4.2. Therefore, archetypes with and without shear-controlled wall segments are assessed within PG1 and PG2, which populate both the FEMA P-58 shear-controlled and flexure-controlled special reinforced shear walls into the performance model. The definition of each performance group is shown in Table 7.

Table 7. Summary of SRMSW performance groups.

Performance Group	Stories	Includes Shear Segments?	Pct. of Shear Controlled Segments
PG1-RM-F	2, 3, 4	No	--
PG1-RM-S		Yes	5, 9, 11, 15, 20, 25, 30, 50, 75, 100%
PG2-RM-F	6, 8, 10, 12	No	--
PG2-RM-S		Yes	5, 9, 11, 15, 20, 25, 30, 50, 75, 100%

2.4. Estimation of Structural Responses

The structural responses for the archetypes were determined using the SP3 Structural Response Prediction Engine (SRPE) (Cook et al. 2018). The SRPE generates a simplified linear multi-degree-of-freedom model representative of strength and stiffness requirements. Nonlinear response is determined by modal analysis, which is subsequently modified to account for the system's nonlinear behavior. The expected nonlinear behavior is calibrated by sampling from

Incremental Dynamic Analysis (IDA: Vamvatsikos and Cornell, 2002) results from high-fidelity nonlinear models of special SRMSW buildings. The SRMSW SRPE was developed as part of the RDC qualification of SRMSW systems for the Concrete Masonry and Hardscapes Association (CMHA).

The following sections provide an overview of the analytical basis behind the SRPE and the quantification of different Engineering Demand Parameters (EDPs). This section focuses on the prediction of median response conditioned on spectral acceleration (Sa). Record-to-record uncertainty and modeling uncertainty are modeled according to FEMA P-58 (FEMA, 2018b).

2.4.1. Analytical Basis Behind the SRMSW SRPE in SP3

This section provides an overview of the nonlinear modeling and analysis conducted to develop the SRPE for the SRMSW system. The current draft provides explicit details on the archetype designs and nonlinear modeling, rather than the forthcoming final report on the SRMSW SRPE development. Later versions of this report will condense this section when the final SRPE report is available.

The SRCSW SRPE is based on calibration to a subset of 4 buildings from the NIST FEMA P-695 implementation study (NIST, 2010) and 5 buildings from the FEMA P-2139/ATC-116 Project, which specifically examined the collapse analysis of short-period buildings (FEMA, 2020).

The NIST (2010) buildings, referred to herein as “N695”, have residential/hospitality plan configurations ranging from 2 to 12 stories (see Figure 8). All designs are fully grouted walls and assumed seismic design category (SDC) D_{max}, as defined in FEMA P-695 (FEMA, 2009). Designs comply with the strength design procedure in TMS 402-08. Walls are designed and detailed to have non-interactive corner details without coupling participation of the floor system. The structural system consists of longitudinal corridor walls, transverse party (e.g., shared) walls, and gravity framing. An example plan layout is shown for a 4-story design in Figure 7, noting that the plan area does not change across archetypes, but the number of walls varies depending on the building height. Typical building elevations are shown in Figure 8, noting that the N695 designs have a constant story height of 10 feet. The floor system consists of a 5-inch cast-in-place slab in corridor areas and 8-inch precast hollow-core planks with a 2-inch topping elsewhere. The directional nature of the flooring system creates low and high wall gravity loads in the longitudinal and transverse directions, respectively (see Figure 7). Walls have a constant length of 32 feet, yet reinforcement ratios, masonry thickness, and masonry compressive strength vary with building height and wall orientation (i.e., gravity load). Design details for N695 archetypes can be found in the original report (NIST, 2010).

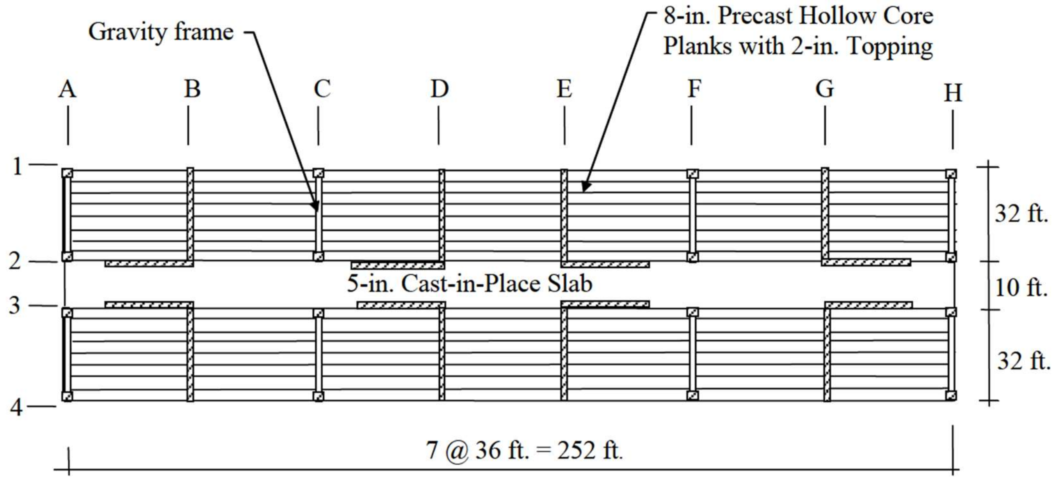

Figure 7 – Typical plan layout for an N695 archetype (4-story design shown). Note that the number of walls varies for different building heights (NIST, 2010).

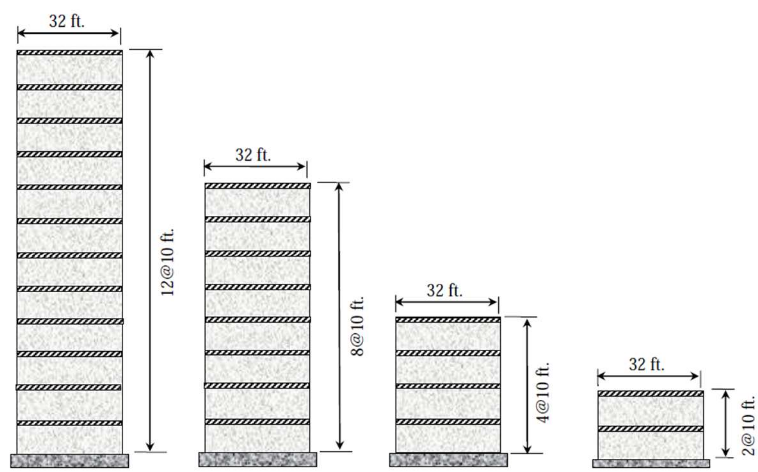

Figure 8 – Elevation views for N695 archetypes (NIST, 2010)

The FEMA P-2139 designs (FEMA, 2020), referred to herein as "P2139", have a commercial plan configuration consisting of corner flange walls and rectangular walls with pilasters in the longitudinal direction (see Figure 9). The P2139 designs are 1, 2, and 4 stories. Three designs (COM1, COM2 and COM3) are designed to SDC D_{max}, as defined in FEMA P-695 (S_{DS} = 1.0, S_{D1} = 0.6). Two designs (COM5 and COM6) are designed to SDC E (S_{DS} = 1.5, S_{D1} = 0.9). Walls were designed using the strength design approach in TMS 402-13. Corner walls are designed as flanged walls and coupling effects due to the floor system are neglected. The floor system consists of concrete topped metal deck for typical floors and an un-topped steel deck supported by open steel joists at the roof level. All story designs have a constant story height of 12 feet and assume a 24-inch (3 block courses) parapet above roof level, as shown in Figure 9. Gravity loads are carried by walls, steel beams and steel gravity columns. A typical floor wall and framing layout is shown in Figure 10. Wall lengths vary based on building height and SDC. The wall layout shown in Figure 10 is representative of all designs except P2139-COM6 (4-story, SDC E), which has two additional rectangular walls acting in the East-West direction at the locations of exterior gravity columns in Figure 10 (i.e., centered at grid lines 2 and 4). Wall lengths, reinforcement ratios, masonry thickness, and specified masonry compressive strength vary based on building height and SDC. Explicit design details can be found in the FEMA P-2139-3 report (FEMA, 2020).

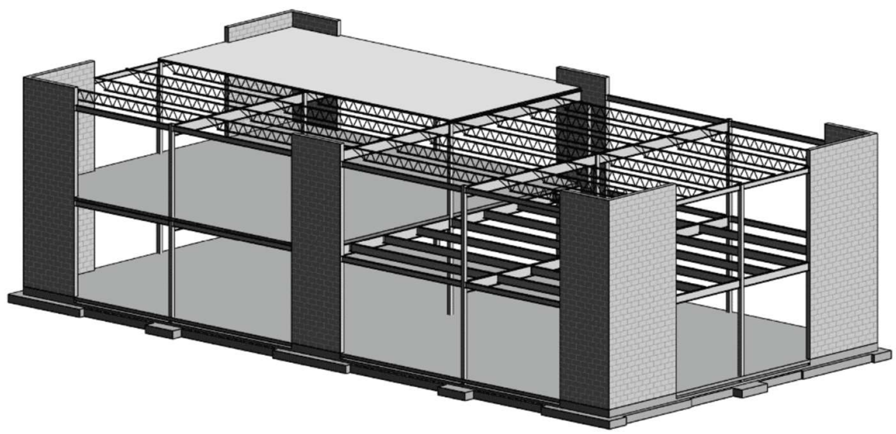

Figure 9 – Isometric view of two-story P2139-COM2 design (FEMA, 2020)

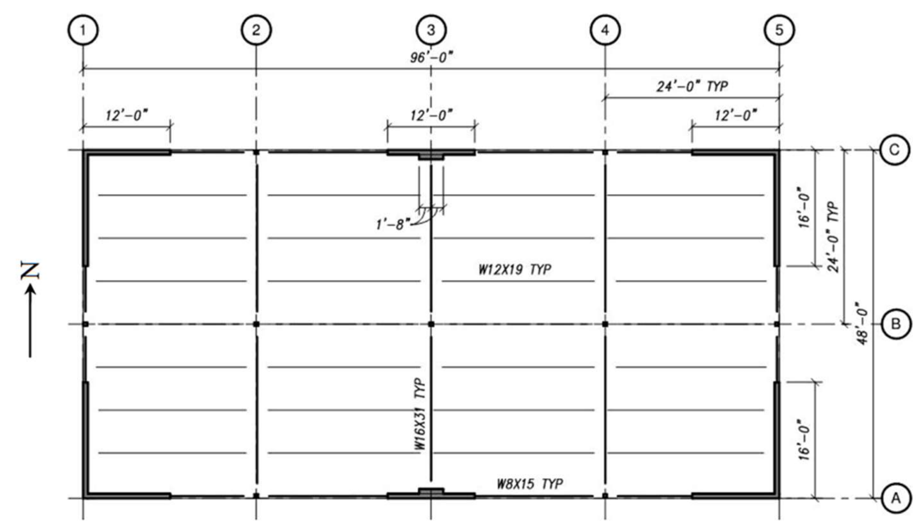

Figure 10 – Framing plan of four-story P2139-COM3 design (FEMA, 2020)

The nine building designs considered were used to develop 18 different 2D building models in *OpenSees* (McKenna et al. 2010). The N695 buildings were modeled using the "low axial load" and "high axial load" wall designs separately (8 archetype models). The P2139 buildings were modeled as the East-West and the North-South directions (10 archetype models).

N695 models are idealized as isolated cantilevers of a single wall location, consistent with the original study (NIST, 2010). P2139 models are idealized as wall piers acting in a single direction with tributary lateral mass corresponding to half the plan area (see Figure 10). Local gravity load assumptions are consistent with the parent studies, and verified through comparison with reported axial load ratios (N695 models) or an example model provided by the original analyst behind FEMA P-2139-3 (Jianyu Cheng, UCSD). P2139 models assume a *rigidDiaphragm* constraint at floor and roof levels.

The modeling of wall elements is conducted using Multiple Vertical Line Elements (*MVLEM*) that consist of two structural nodes defining the vertical section of a wall with uniaxial macro fiber elements in series with a shear element allowing for the wall section to be defined (Kolozvari et al. 2015; Orakcal et al. 2004; Vulcano et al. 1988). An illustration of a MVLEM element is shown in Figure 11.

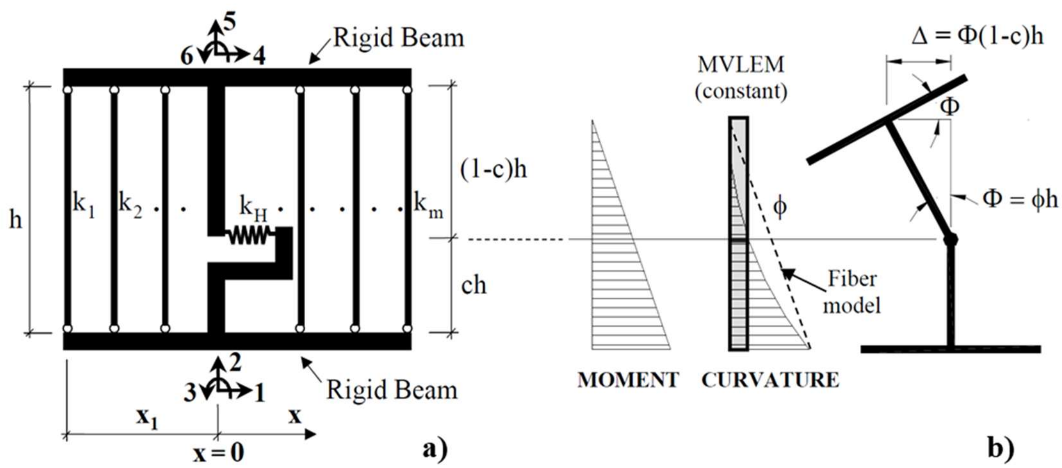

Figure 11 – MVLEM element: a) model element formulation; b) rotations and displacements (Kolozvari et al., 2015)

The material properties used for modeling the flexural and shear behavior of SRMSW explicitly follow the NIST Modeling Guidelines for flexure-controlled RM walls using fiber elements (NIST, 2017) that is the basis for the recently updated backbone curves in ASCE 41-23 (ASCE, 2023) for flexure-controlled RM walls. These updates are based on data synthesis (Cheng and Shing, 2018; Cheng, 2021; Cheng and Shing, 2022) of available experimental testing (e.g., Shedid et al. 2008; Shing et al. 1991; Sherman, 2011; Ahmadi, 2012; Kapoi, 2012). Although more complex modeling procedures have been published for RM shear walls (e.g., Mavros, 2015; Koutras, 2019; Cheng and Shing, 2022b), the adopted modeling scheme is assumed to be well in-line with the current state of practice. Uniaxial behavior (flexure) of masonry is modeled using the *Concrete01* material in *OpenSees* (Kent and Park, 1971) with a peak compressive strain of -0.003 (Atkinson and Kingsley, 1985) with zero tensile stress. Uniaxial behavior of reinforcement is modeled using the *Hysteretic* material in *OpenSees*. The reinforcement material considers buckling in compression and fracture under cyclic tension, per NIST (2017) and Cheng and Shing (2022). The strain at compressive buckling, ε_b, corresponds to 40% post-peak strength of the masonry. The strain at the onset of cyclic fracture in tension, ε_{ps}, is a function of the reinforcement index ($\alpha = f_y\rho_v/f_m$) and axial load ratio ($\beta = P/f_mA_n$). An illustration of the material backbones used to model the flexural response of RM walls is shown in Figure 12.

The effective plastic hinge length, L_p, is assumed to be 20% of the wall height (NIST, 2017). One- and two-story models explicitly model the plastic hinge length by providing two MVLEM wall elements within the first story, producing the case where the modeled plastic hinge length (L_e) is equal to L_p. Taller buildings (greater than 2-story) model the plastic hinge as the first story height (i.e., $L_e \neq L_p$). For these cases, the flexural fiber materials (see Figure 12) are adjusted to maintain objectivity of strain localization (Bažant and Oh, 1983; Jansen and Shah, 1997; Coleman and Spacone, 2001). NIST (2017) provides guidance on implementing these adjustments for the current uniaxial material models.

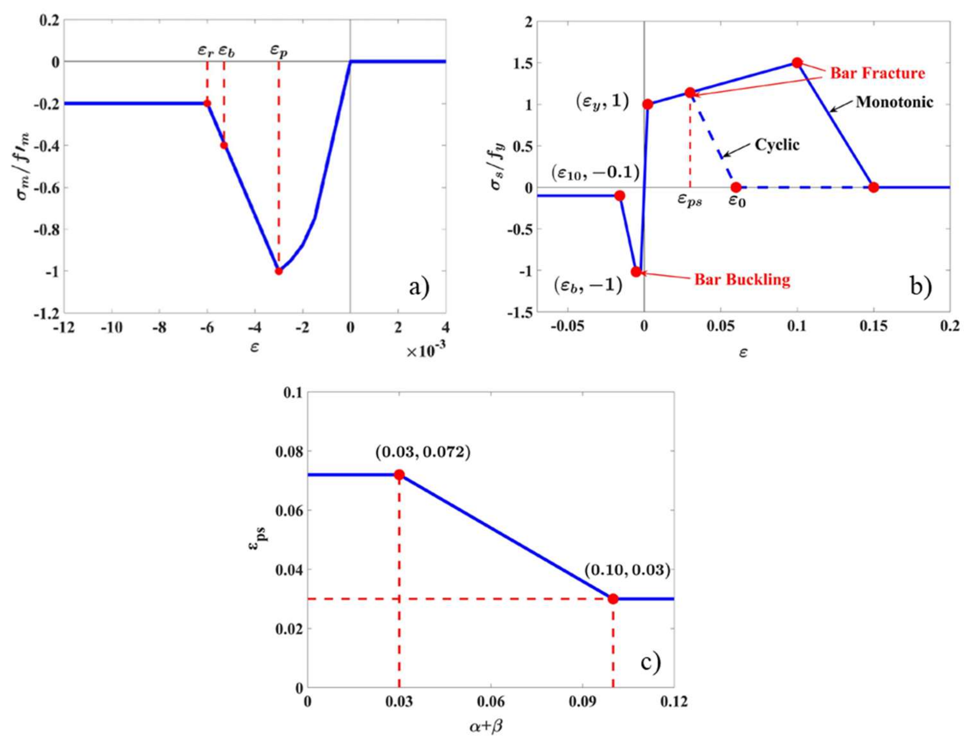

Figure 12 – Material backbones used for flexural fiber modeling: a) Normalized stress-strain for masonry; b) Normalized stress-strain for reinforcement (including buckling and cyclic fracture); c) Tensile strain at cyclic bar fracture as a function of reinforcement index (α) and axial load ratio (β). Images adapted from Cheng and Shing (2022).

Fiber sections are discretized with 2-inch cover fibers (toe of wall) and 4-inch interior fibers (approximate size of a grout cell) for rectangular walls. Flanged walls are similarly discretized, yet with two 1-inch cover fibers on the end of the wall where the flange is loaded in compression. MVLEM elements require that the reinforcement ratio relative to the area of the current fiber be specified. Reinforcement layouts provided by the parent studies were followed explicitly when developing fiber section for RM walls.

Shear behavior is modeled as effective (cracked) elastic both within the plastic hinge region and in upper stories. Flexure behavior of wall elements outside of the plastic hinge region are modeled as effective elastic. Effective flexural and shear stiffness use the suggested modifiers in ASCE 41-23 (i.e., ζ_f and ζ_v) for rectangular and flanged wall sections. Flanged wall sections assume the average value between flange in compression and flange in tension. Effective flange lengths are taken as the controlling case (smaller value) for flange in tension and compression according to TMS 402/602-16. This results in assuming three and four 16-inch-long units are effective for 8-inch and 12-inch-thick walls, respectively, for flanged walls.

Second order effects (P-Delta) are accounted for using a leaning column with a *PDelta* geometric transformation in *OpenSees*. The entire gravity load, including local wall loads, are applied to the leaning column since MVLEM elements do not account for second order effects (Terzic and Kolozvari, 2020). Inherent damping is applied as 5% initial stiffness proportional Rayleigh damping. Target damping is applied to the elastic first and third mode periods (i.e., T_1 and T_3). 2-story models apply damping at the first and second modes. One-story models assume T_1 and $1.5T_1$ as Rayleigh periods. Mass proportional damping is applied to all sources of mass in the models. Stiffness proportional damping is only applied to linear elastic elements (i.e., not applied to MVLEM elements representing plastic hinge regions). This is to avoid complications associated with using initial stiffness proportional damping in nonlinear elements (Hall, 2006; Charney, 2008; Chopra and McKenna, 2016).

All models were analyzed using the FEMA P-695 far-field ground motion set (FEMA, 2009), consisting of 44 ground motions (i.e., 22 horizontal pairs). Incremental Dynamic Analysis (IDA: Vamvatsikos and Cornell, 2002) was used to obtain a range of linear and nonlinear structural responses for calibration.

2.4.2. *Structural Properties Estimation*

Building structural properties are estimated using a linear building model, with strength and stiffness scaled to meet corresponding design requirements. Typical levels of overstrength (e.g., due to expected material properties, etc.) are added after design requirements are satisfied, to provide the best possible estimate of the true strength and stiffness of the LFRS. The commercial version of SP3 also includes additional strength and stiffness contributions from the gravity system and nonstructural components, but these are excluded in this study for compliance with the procedures of Section A.8 of the 2026 NEHRP Provisions.

The process begins by determining the design parameters, including spectral values, response modification factor (R), deflection amplification factor (C_d), and related values (e.g., I_e). Next, a target seismic design drift is selected. For drift-controlled systems, such as most moment frames, this target is typically the design drift limit—for example, 2% for risk category II buildings. For strength-controlled systems, the target drift is a realistic value appropriate for the system type and building height; the expected design drift values are based on a database of hundreds of building designs (from archetype buildings in the SP3 SRPE database). Resilient design iterations use the same process with pairs of R_{fr} and Δ_{afr} for a given analysis. Notably, the deflection amplification factor for functional recovery (C_{dfr}) is taken equal to R_{fr}, and the building importance factor (I_e) is taken as unity per Section A.8 of the 2026 NEHRP Provisions.

Following this, the period of a representative design model (limited to the LFRS) is determined, considering the target seismic drift and stability requirements (ASCE 7-22 Section 12.8.7). This involves constructing a simple multi-degree-of-freedom (MDOF) model that reflects the system's mass and stiffness characteristics. For instance, moment frames tend to be more shear-dominated, whereas walls and braced frames are more flexure-dominated. This approach is based on a method developed by Miranda (1999) and Miranda and Reyes (2002) but utilizes matrix structural analysis with mass and stiffness matrices rather than purely analytical equations; it also incorporates the ability to model rotational flexibility at the base.

Starting with very low stiffness, the stiffness matrix is systematically scaled (i.e., increased) until the model achieves the target drift or less, while also satisfying stability requirements. Generally, modal response spectrum analysis (MRSA) is used to generate structural properties for buildings that are modern code-compliant, taller than four stories, and located in high or very high seismic areas. For other cases, the equivalent lateral force (ELF) procedure is used. Wind drift checks can be included in this step but were omitted for this study.

Next, the expected strength and stiffness of the LFRS are determined, accounting for overstrength. These properties vary depending on the LFRS type and building height and are calibrated using results from OpenSees models and engineering judgment. An additional optional check can be performed to ensure compatibility between strength and stiffness. If the stiffness is found to be too high or low in relation to the strength and yield drift, it is adjusted to a reasonable level. The final estimates of the first three periods and mode shapes of the building are determined by performing an eigen analysis with the stiffness matrix and mass matrix. The final estimate of the ultimate base shear strength is determined from design strength and the expected overstrength.

Where shear critical walls are included in the model, the strength is adjusted to account for the requirements that shear critical walls are designed for 2.5 times the design shear demand. Therefore, the strength of the building is a function how much of the LFRS is shear critical, using the equation:

$$V_{SC} = V_{FC}[1 + (2.5 - 1)F_{SC}]$$

where V_{SC} is the estimated strength considering additional required strength of shear-critical walls. V_{FC} is the estimated strength of a fully flexure-controlled design. The term F_{SC} represents the fraction of walls that are shear-critical (ranging from 0.05 to 1.0 in the archetype space).

2.4.3. Story Drift Ratio

The SRMSW SRPE estimates peak story drift ratio at each story, accounting for the first three mode shapes and periods of the building and its peak strength. First, peak roof drift ratio is estimated using a method that is similar to the ASCE 41 (ASCE, 2023) method for target roof displacement (Section 7.4.3.3.2), but with factors calibrated directly to the OpenSees model results; it depends on the fundamental building period, modal participation factor, spectral acceleration, and correction factors for nonlinear behavior. Second, linear modal analysis is performed using the first three modes, and the results are scaled so that the roof drift from the first step is reproduced. If the spectral acceleration demand is large enough to cause yielding in the structure, then the story drifts are adjusted to account for nonlinear demands. Nonlinear demands are adjusted based on an intensity factor $S = S_a/(V_{max}/W)$, where S_a is the first mode spectral acceleration and (V_{max}/W) represents the normalized peak strength of the building using expected properties. Larger values of S (i.e., more damage) result in more drift concentration in the lower stories. The way in which drifts localize as S increases is calibrated to the nonlinear modeling results and depends on the height of the building (i.e., number of stories) and the type of structural system. An example calibration for a 12-story RC special moment frame model is shown in Figure 13. The solid lines represent the median peak drift profile from nonlinear time history analysis (NRHA) compared to SRPE response shown in thicker dashed lines. The dotted lines show the elastic response profile before adjusting for nonlinear behavior.

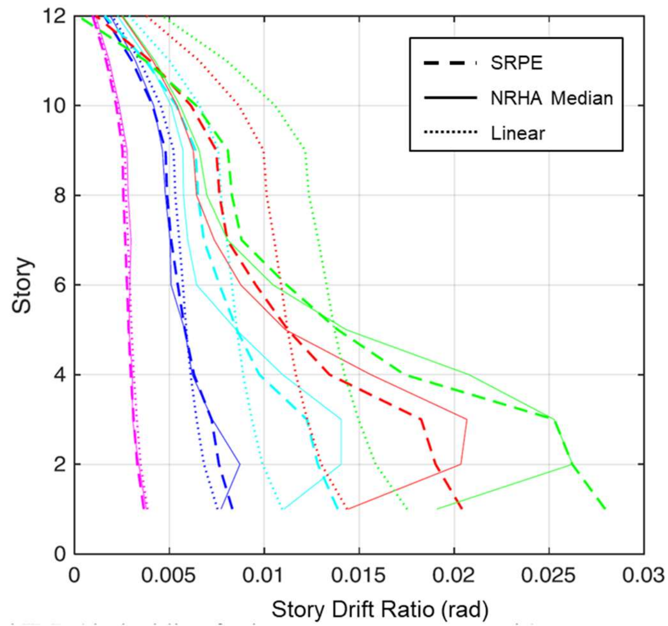

Figure 13. Comparison of SRPE (dashed) and median NRHA (solid) story drift ratio response for a 12-story RC special moment frame. Note, dotted lines represent predicted linear response prior to adjustment for nonlinear behavior. Figure adapted from Cook et al. (2018).

2.4.4. Wall Chord Rotation

The chord rotation at the base of the wall is estimated by converting the SRPE story drift profile to a global displaced shape. This conversion includes an adjustment factor to convert the peak story drift profile to a peak transient drift profile since the peak drift does not occur simultaneously at each level, especially for taller buildings. The global rotation at the first mode effective height is taken as the total chord rotation demand at the wall base. An illustration of this calculation is shown in Figure 14, where θ_{wall} represents the wall chord rotation at the base. This approximation of wall chord rotation aims to maintain consistency with the development of fragility functions (see Section 2.2.1) while relying on the story drift calibration to adequately capture differences in building height.

The chord rotation demand at upper stories is not as critical for estimating wall damage; these values are numerically calibrated to nonlinear models as ratios of the base chord rotation. The chord rotation at upper levels tends to be nearly an order of magnitude lower than the base chord rotation. An example response calibration plot is shown in Figure 15.

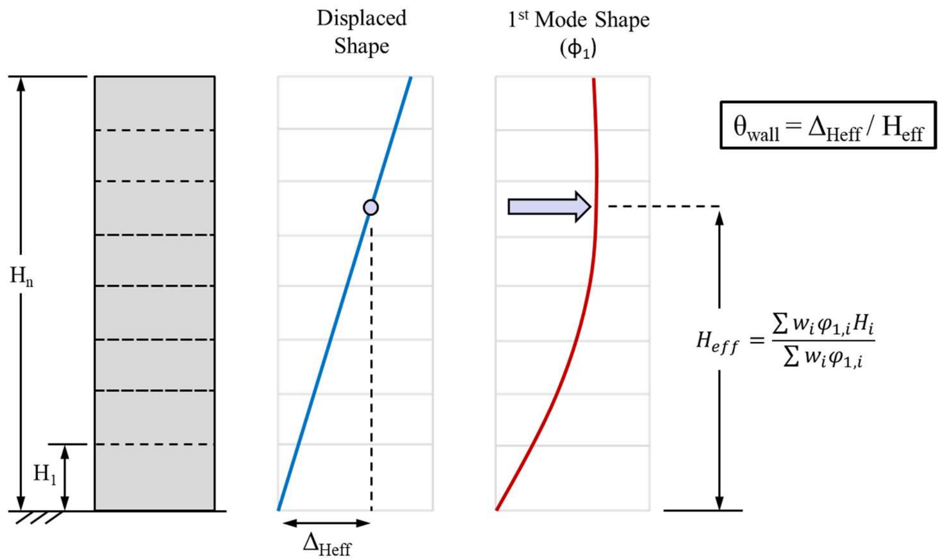

Figure 14. Illustration of using the displacement at the first mode effective height to approximate the total chord rotation at the base of SRMSWs .

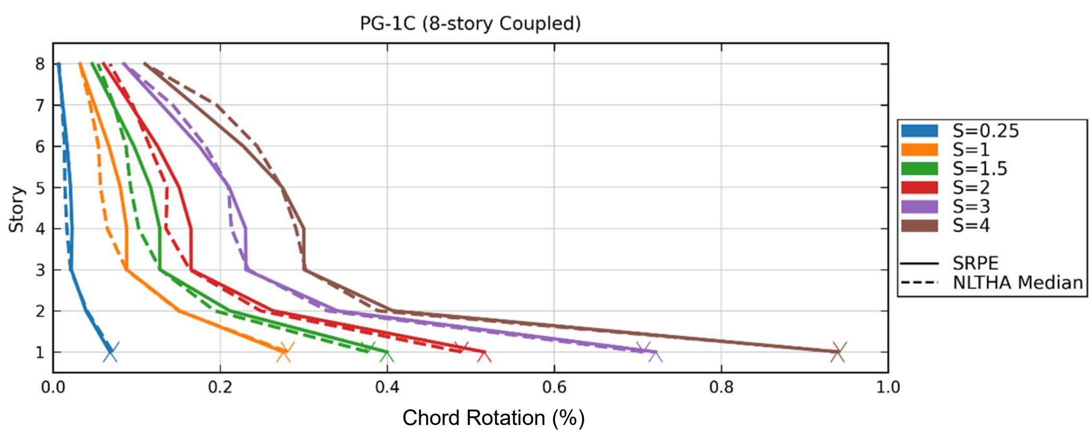

Figure 15: Comparison of SRPE (solid) and median NRHA (dashed) peak chord rotation response for an 8-story Coupled SpeedCore wall. The various "S" values are different levels of inelasticity ($S=Sa(T_1)/v_{ult}$). Figure adapted from Almeter et al. (2024).

2.4.5. Peak Floor Acceleration

Peak floor acceleration (PFA) is computed based on spectral acceleration, building strength, and the first three modal periods and shapes of the building. First, elastic PFA is computed with modal time-history analysis using the FEMA P-695 far-field record set scaled to the intensity of interest. Then, if the spectral acceleration demand is large enough to cause yielding, PFA is adjusted using the intensity factor $S = S_a/(V_{max}/W)$. The amount of reduction of the response depends on how high the story is above the ground, because damage in the lower stories "isolates" the upper stories from acceleration input. An example calibration for a 12-story RC special moment frame model is shown in Figure 16. The solid lines represent the median PFA profile from NRHA compared to the SRPE response shown in thicker dashed lines. The dotted lines show the elastic response profile before adjusting for nonlinear behavior. Note that the largest intensity shaking (green lines) has significant reductions in PFA at upper stories due to damage in the lower stories.

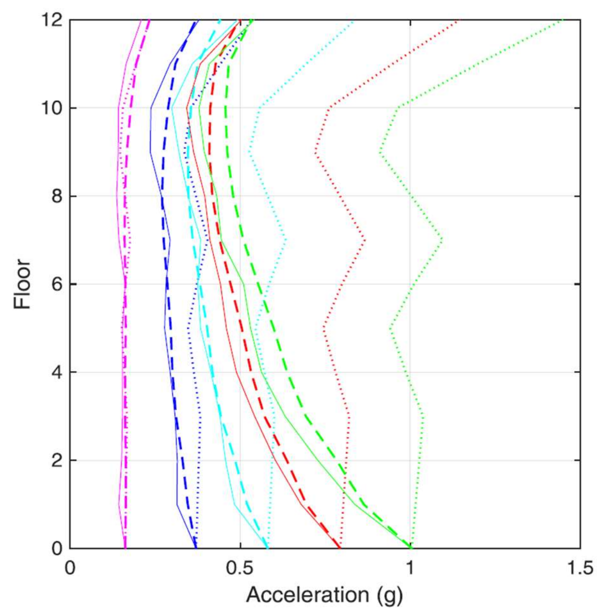

Figure 16. Comparison of SRPE (dashed) and median NRHA (solid) peak floor acceleration response for a 12-story RC special moment frame. Dotted lines represent predicted linear response before adjustment for nonlinear behavior. Figure adapted from Cook et al. (2018).

2.4.6. Treatment of Residual Drift Ratio

The FEMA P-58 residual drift model was updated during the ATC-138 project (ATC, 2021) and resulted in a supplemental FEMA P-58 background document *BD 3.7.26: Updated Model and Criteria for Residual Drift* (DeBock et al. 2024). The revisions to the original FEMA P-58 model allowed for distinctions between structural systems, based on recent analytical studies (Almeter et al. 2018; Vouvakis Manousakis et al. 2024).

The median residual story drift ratio (Δ_r) is estimated from the median transient story drift ratio (Δ) and yield drift ratio (Δ_y). The general format for simplified residual drift estimation has a trilinear form with a transition slope and a primary slope. The initial slope represents the elastic response range (i.e., $\Delta \leq \Delta_y$) where residual displacement is not expected. The transition slope reduces the rate of residual drift accumulation in the region just beyond elastic response to a specified drift ductility, after which, the steeper primary slope accumulates residual drift at a faster rate as peak drift demands increase. The end of the transition region is defined by a system specific drift value Δ_{shift}. An illustration of the basic components of the trilinear residual drift model is shown in Figure 17.

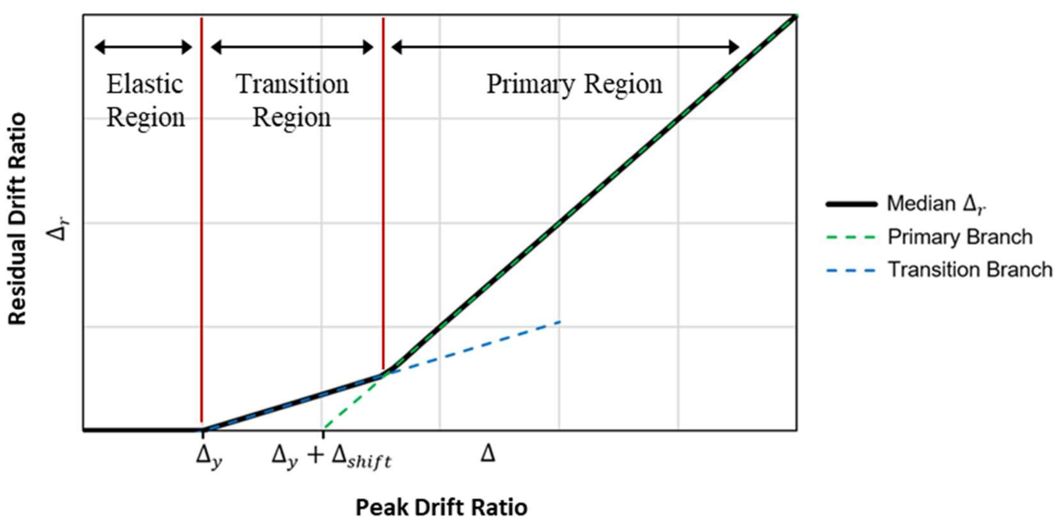

Figure 17 – Basic components of the trilinear model to estimate residual story drift as a function of peak story drift demand and yield story drift.

Three residual drift models were developed as part of the FEMA P-58 revisions, with parameters summarized in Table 8. For masonry shear wall systems, the generalized inelastic residual drift model is selected according to the FEMA P-58 recommendations, as listed in Table 9. The recommended yield drift ratio (Δ_y) for SRMSW systems is 0.25%. The residual story drift ratio as a function of story drift ratio demand for the SRMSW system is shown in Figure 18.

Table 8. Parameters of updated FEMA P-58 residual drift models

Residual Drift Model	Δ_{shift}	Primary Slope (a)	Transition Slope (b)
Steel MRF	0.005	0.5	0.2
BRBF	0.007	0.4	0.1
General Inelastic	0.008	0.35	0.15

Table 9. Recommended yield story drift ratio (Δ_y) and residual drift models by LFRS

LFRS	Δ_y (rad)	Residual Drift Model
Steel MRF	0.01	Steel MRF
Steel CBF	0.003	General Inelastic
Steel EBF	0.005	BRBF
Steel BRBF	0.002	BRBF
RC MF	0.0075	General Inelastic
RC Wall	0.0025	General Inelastic
Masonry	0.0025	General Inelastic
Wood or CFS light frame	0.075	General Inelastic

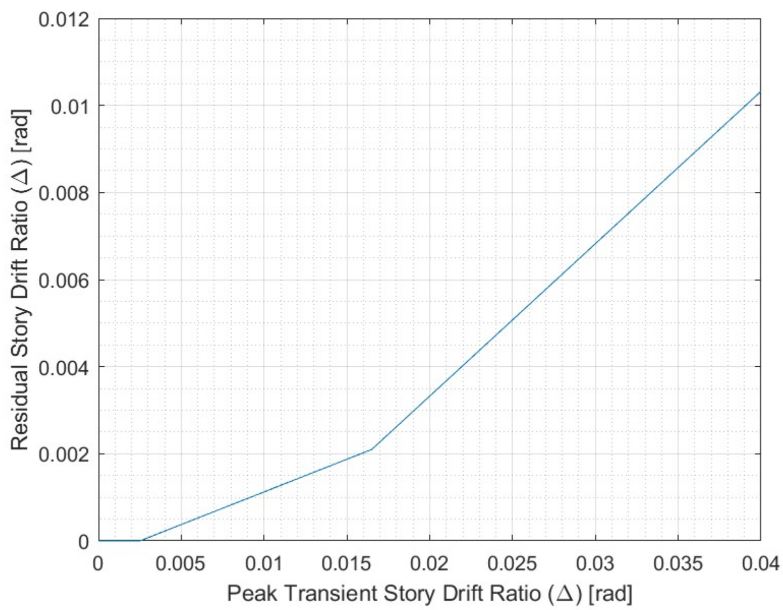

Figure 18. Residual drift model for the SRMSW structural system, based on the general inelastic drift model and a 0.3% yield drift.

3. RESULTS

The tables and plots below show the R_{fr} and Δ_{afr} envelopes for each combination of performance group variants. This design envelope identifies the possible design value combinations where all performance groups satisfy both the max and mean analysis criteria. Results are provided separately for both FRC A/B/C acceptance criteria in Section 3.1 and FRC D acceptance criteria in Section 3.2. Additional figures illustrating general system performance in terms of structural response, component damage, and design features are provided in Section 3.3. Full details on the performance of individual archetypes are provided in the attached supplementary materials.

3.1. FRC A/B/C Analysis Results

Table 10 – R_{fr} values across various allowable drift limits required to satisfy the FRC A/B/C structural performance acceptance criteria for each performance group. Analysis results assume increased strength requirements impact building stiffness.

Perform. Group	Criteria	Δ_{afr}									
		0.001	0.002	0.003	0.004	0.005	0.006	0.007	0.008	0.009	0.01
PG1-RM-F	Max[1]	5	5	5	4	4	4	4	4	4	4
PG2-RM-F	Max[1]	5	5	5	5	4	4	4	4	3.5	3.5
PG1-RM-F	Mean[1]	5	5	4	3.5	3.5	3.5	3.5	3.5	3.5	3.5
PG2-RM-F	Mean[1]	5	5	5	3.5	3*	3	3	3	3	2.5
	Envelope	5	5	5	4	3.5	3*	3	3	3	3

Perform. Group	Criteria	Δ_{afr}									
		0.001	0.002	0.003	0.004	0.005	0.006	0.007	0.008	0.009	0.01
PG1-RM-S	Max[1]	5	4	3	3	3	3	3	3	3	3
PG2-RM-S	Max[1]	5	5	3	2.5	2.5	2.5	2.5	2	2	1.5
PG1-RM-S	Mean[1]	5	4.5	3.5	3.5	3.5	3.5	3.5	3.5	3.5	3.5
PG2-RM-S	Mean[1]	5	5	3.5	3	3	3	3	2.5	2.5	2
	Envelope	5	4	3	2.5	2.5	2.5	2.5	2	2	1.5

[1]In each performance group, the combination of R_{fr} and Δ_{afr} is deemed to be acceptable if the mean P[SCSD] is less than 10%, and the maximum P[SCSD] across all archetypes in the performance group is less than 20%.

*The final selected R_{fr} is higher than the allowable value indicated on this table. However, the selected R_{fr} and Δ_{afr} combination results in a P[SCSD] value that exceeds the acceptance criteria by a justifiably small margin (<2%). Please see Figure 19, which shows that the final selected combination is close to the envelope.

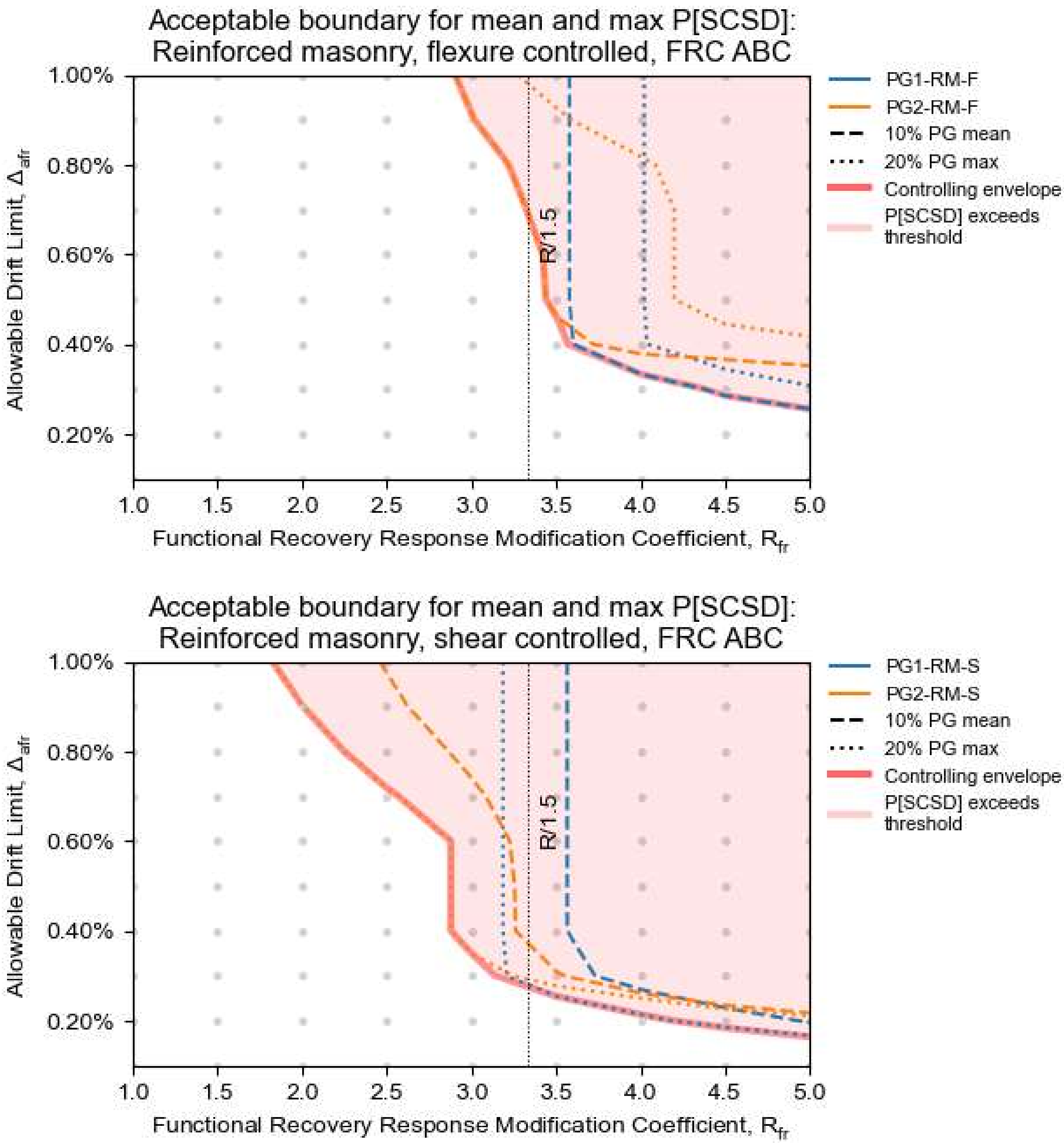

Figure 19 – Combination of R_{fr} and Δ_{afr} values required to satisfy the FRC A/B/C structural performance acceptance criteria for each performance group. Analysis results assume increased strength requirements impact building stiffness.

3.2. FRC D Analysis Results

Table 11 – R_{fr} values across various allowable drift limits required to satisfy the FRC D structural performance acceptance criteria for each performance group. Analysis results assume increased strength requirements impact building stiffness.

Perform. Group	Criteria	Δ_{afr}									
		0.001	0.002	0.003	0.004	0.005	0.006	0.007	0.008	0.009	0.01
PG1-RM-F	Max[1]	5	5	5	4	4	4	4	4	4	4
PG2-RM-F	Max[1]	5	5	5	5	4.5	4.5	4.5	4.5	4.5	4
PG1-RM-F	Mean[1]	5	5	5	3.5	3.5*	3.5	3.5	3.5	3.5	3.5
PG2-RM-F	Mean[1]	5	5	5	5	4	3.5	3.5	3.5	3.5	3.5
	Envelope	5	5	5	5	3.5	3.5*	3.5	3.5	3.5	3.5

Perform. Group	Criteria	Δ_{afr}									
		0.001	0.002	0.003	0.004	0.005	0.006	0.007	0.008	0.009	0.01
PG1-RM-S	Max[1]	5	4.5	3	3	3	3	3	3	3	3
PG2-RM-S	Max[1]	5	5	3.5	3	3	3	2.5	2	2	1.5
PG1-RM-S	Mean[1]	5	5	4	3.5	3.5	3.5	3.5	3.5	3.5	3.5
PG2-RM-S	Mean[1]	5	5	4	3.5	3.5	3.5	3.5	3	3	2.5
	Envelope	5	4.5	3	3	3	3	2.5	2	2	1.5

[1]In each performance group, the combination of R_{fr} and Δ_{afr} is deemed to be acceptable if the mean P[SCSD] is less than 15%, and the maximum P[SCSD] across all archetypes in the performance group is less than 25%.

*The final selected R_{fr} is higher than the allowable value indicated on this table. However, the selected R_{fr} and Δ_{afr} combination results in a P[SCSD] value that exceeds the acceptance criteria by a justifiably small margin (<2%). Please see Figure 20, which shows that the final selected combination is close to the envelope.

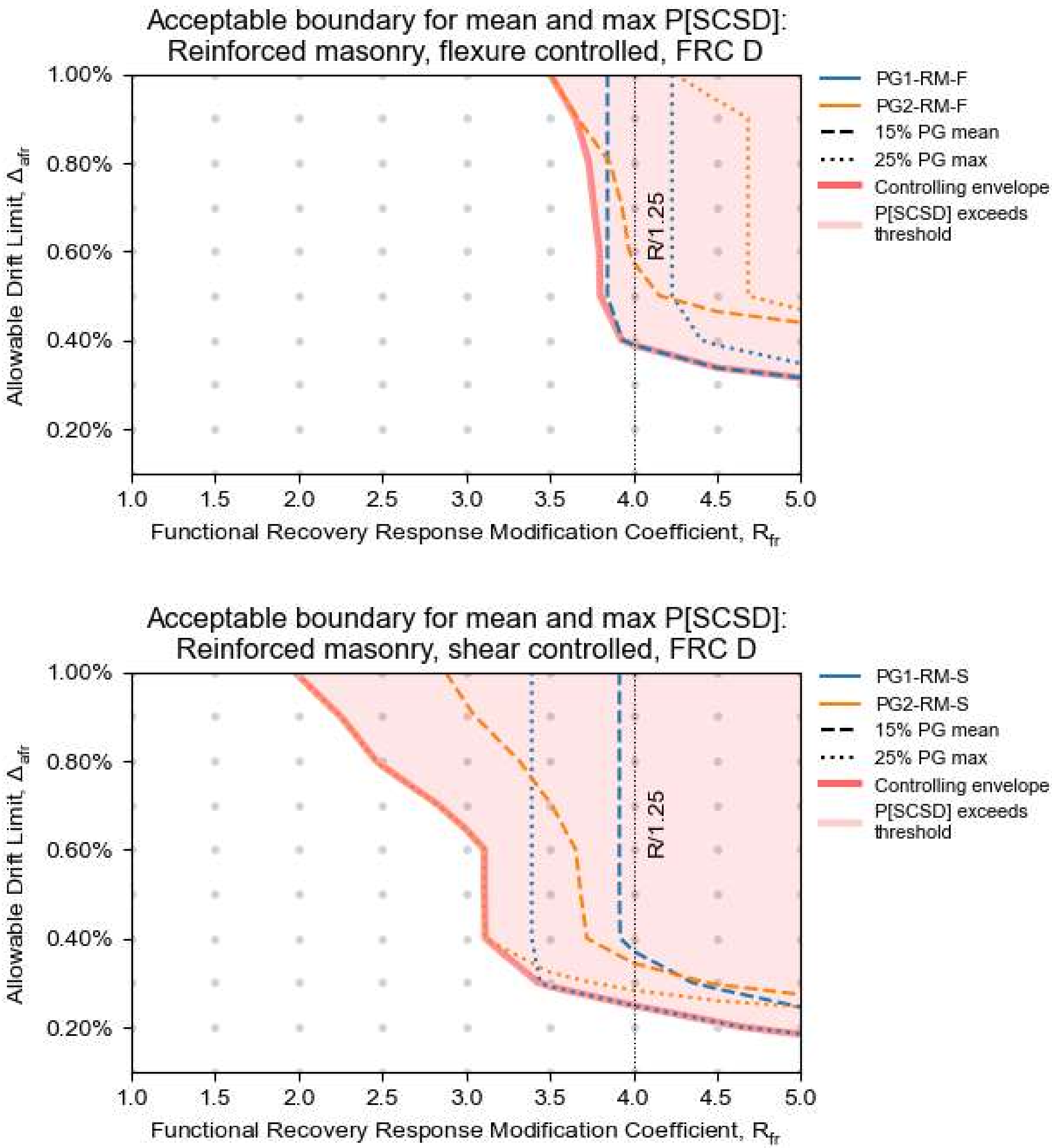

Figure 20 – Combination of R_{fr} and Δ_{afr} values required to satisfy the FRC D structural performance acceptance criteria for each performance group. Analysis results assume increased strength requirements impact building stiffness.

3.3. System Response

The figures below provide detailed insights into the general responses and performance outcomes of the models in each performance group. Figure 21 shows how design drift (Δ_{afr}) relates to median realized drift (x-axis), and how realized drift relates to P[SCSD] (y-axis). The median realized drift is the median peak story drift, in a given story, from all the realizations of peak story drift (~2,000) simulated as part of the FEMA P-58 Monte Carlo assessment. Figure 22 and Figure 23 further break down SCSD contributions by structural component type and show that wall damage is dominant across many performance results for SRMSW buildings. Finally, Figure 24 and 24 shows the transition from strength-controlled to stiffness-controlled design for various R_{fr} and Δ_{afr} combinations. All results presented in this section are general to the response of the system and not specific to the Functional Recovery Category.

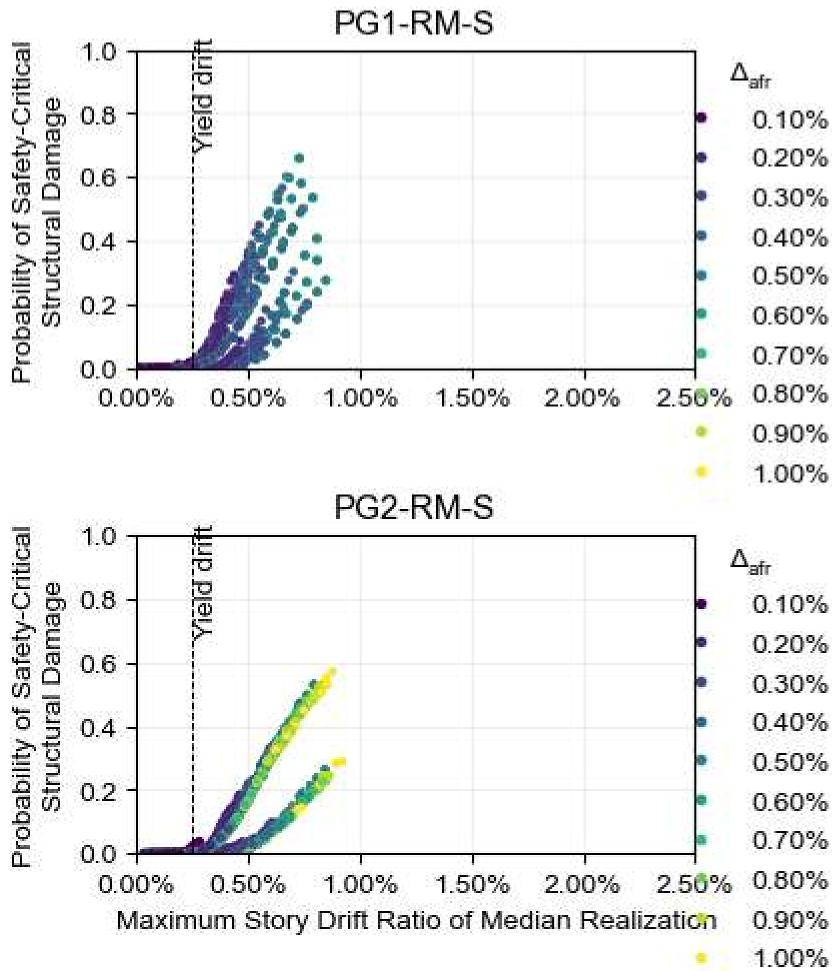
PG1-RM-S
Probability of Safety-Critical Structural Damage
Yield drift
Δ_{afr}
0.10%
0.20%
0.30%
0.40%
0.50%
0.60%
0.70%
0.80%
0.90%
1.00%
PG2-RM-S
Maximum Story Drift Ratio of Median Realization

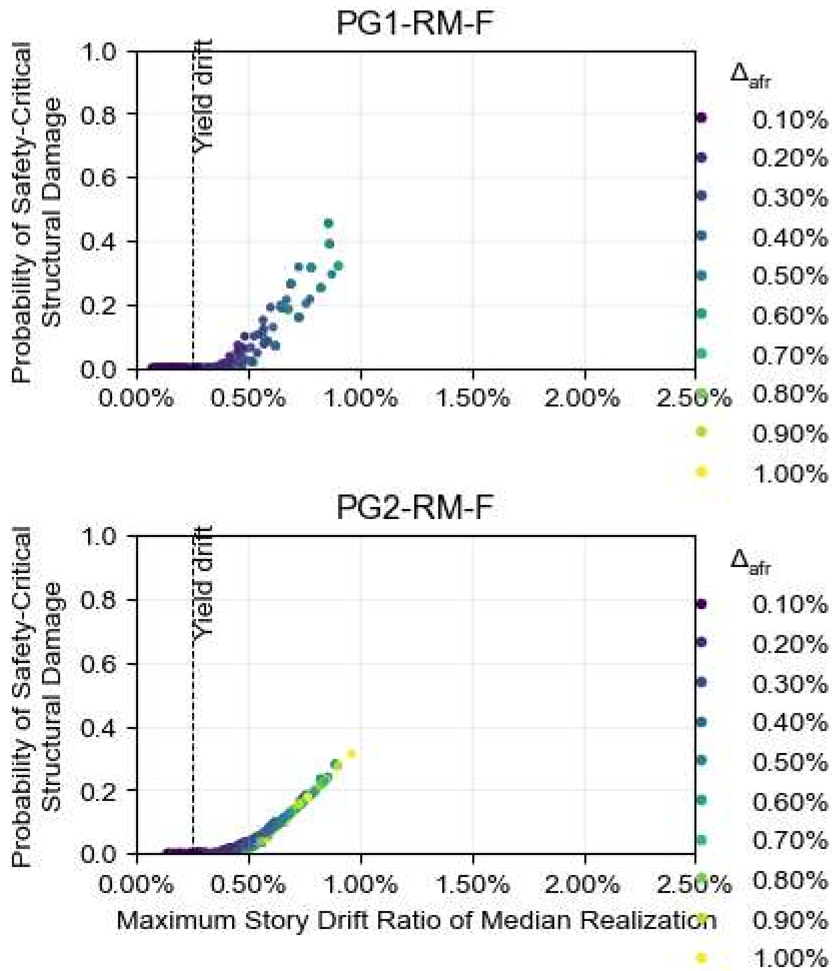

Figure 21 - Relationship between peak realized drift (median) and P[SCSD] for all archetypes.

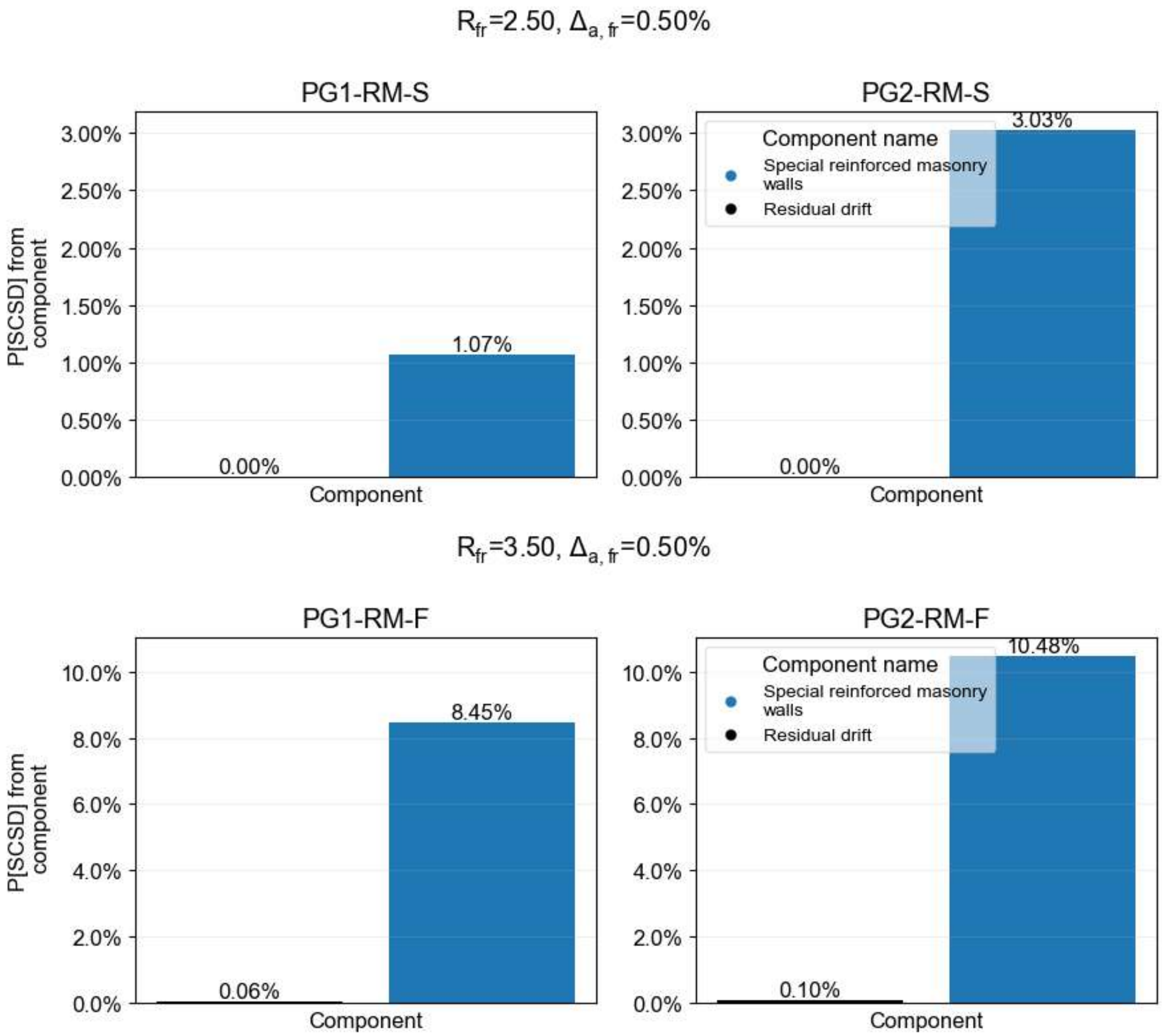

Figure 22 – Component damage contribution to P[SCSD] for each performance group at the recommended design points for FRC ABC

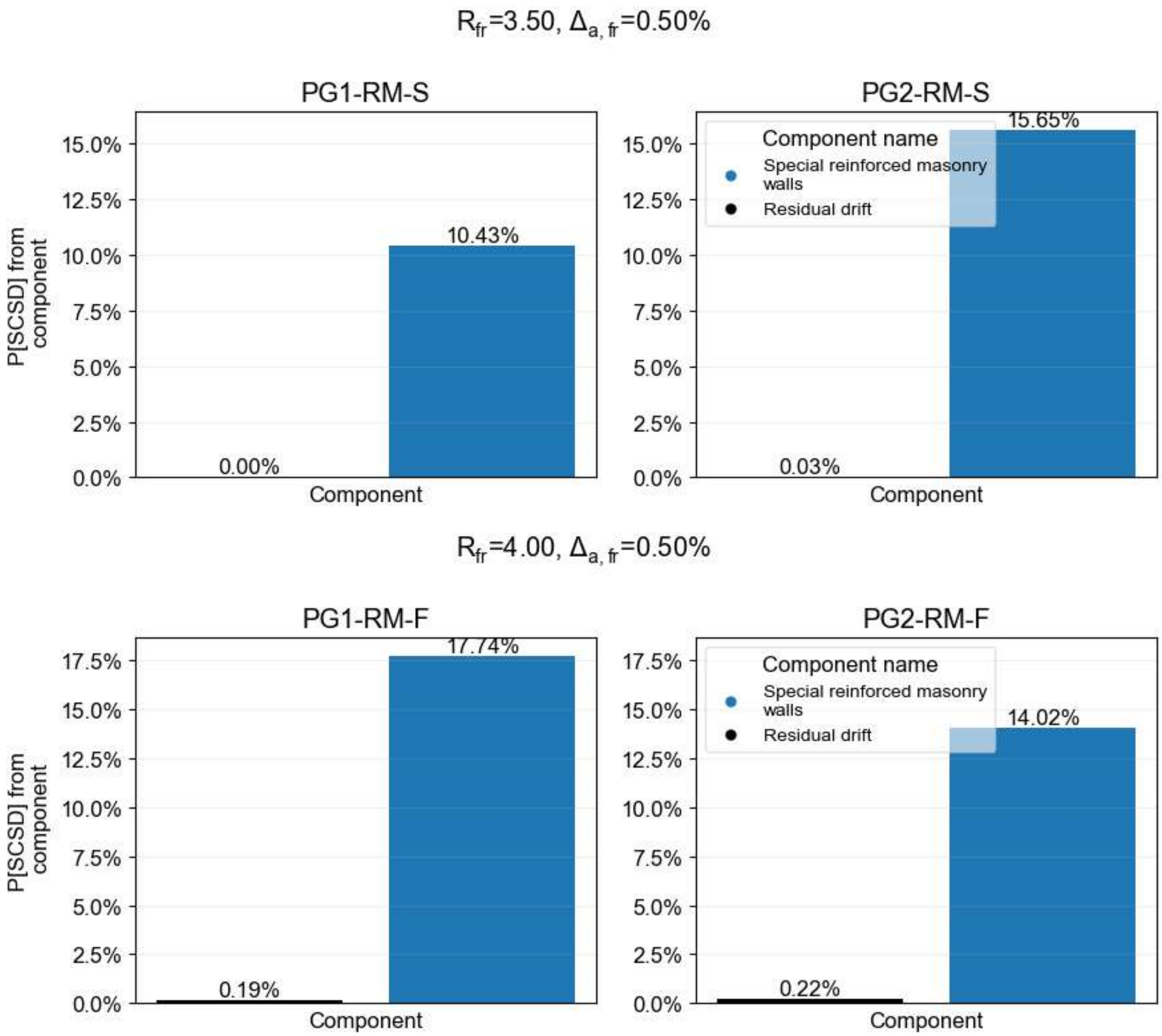

Figure 23 – Component damage contribution to P[SCSD] for each performance group at the recommended design points for FRC D

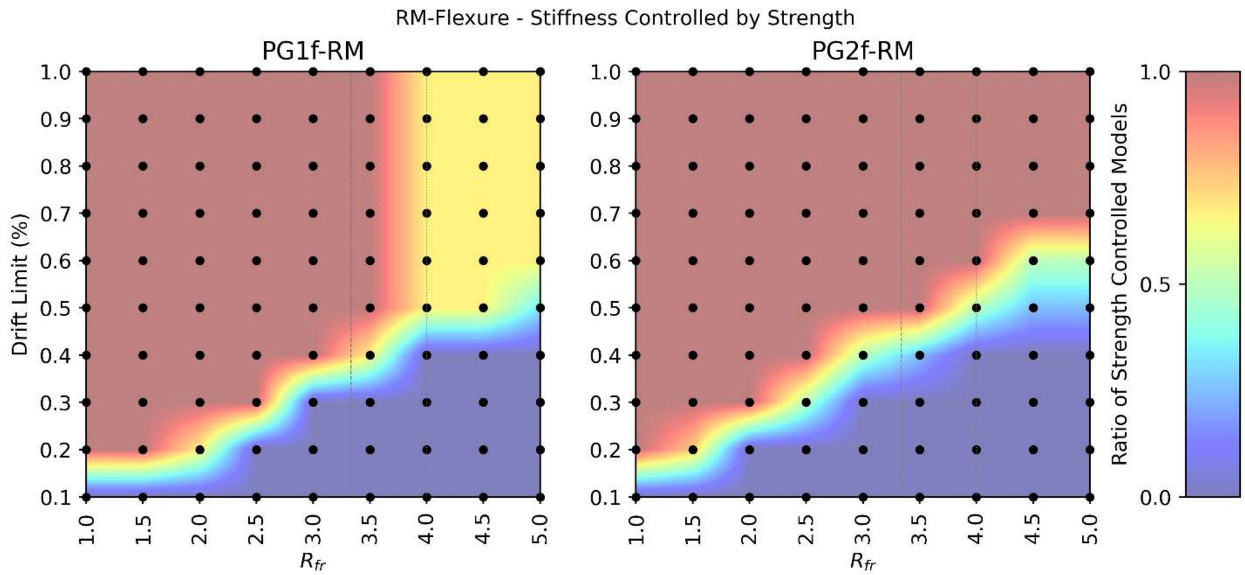

Figure 24 – SRMSW flexure: Average influence of strength on building stiffness for various design requirement combinations assessed. Red coloring indicates that 100% of the models at this design point are controlled by strength requirements (e.g., tightening drift limits by one increment will not change performance). Blue coloring indicates that stiffness requirements control 100% of the models at this design point.

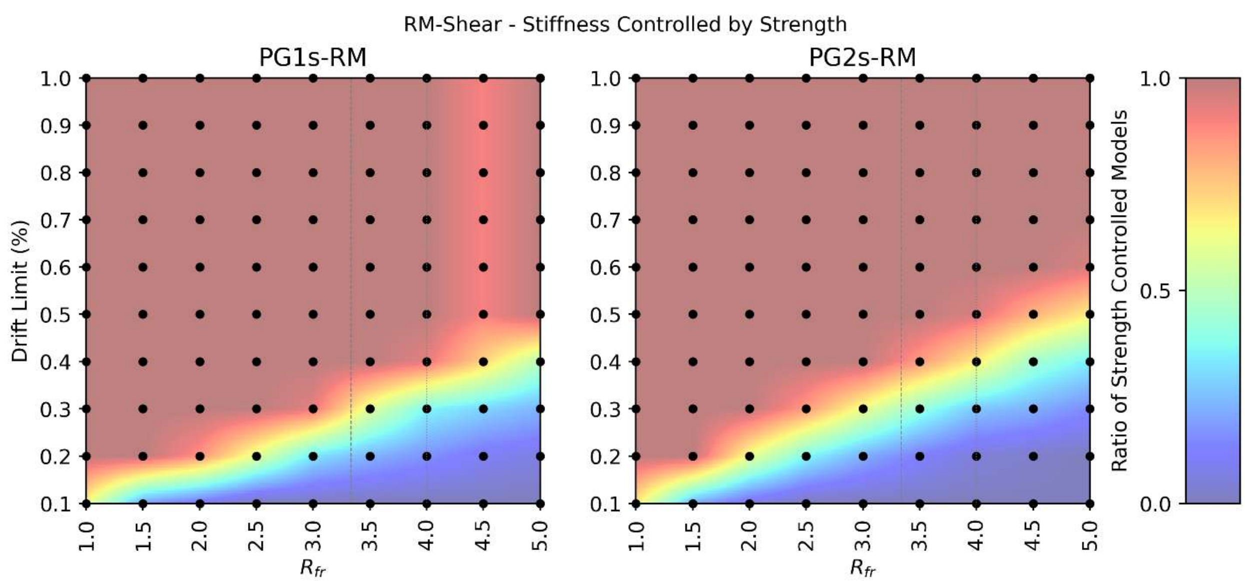

Figure 25 – SRMSW shear: Average influence of strength on building stiffness for various design requirement combinations assessed. Red coloring indicates that 100% of the models at this design point are controlled by strength requirements (e.g., tightening drift limits by one increment will not change performance). Blue coloring indicates that stiffness requirements control 100% of the models at this design point.

3.4. Validation of Peak Floor Acceleration Demand Estimates

The prequalification method documented in the 2026 NEHRP Section A.8.3.6 requires that the peak floor acceleration demands be evaluated for all of the structural system archetype design cases, to ensure that the Section A.10.6 peak floor acceleration adequately reflect the actual peak floor acceleration values observed in the nonlinear response-history analysis results. If the peak floor acceleration demands exceed the acceptable limits of Section A.8.3.6, the recommended $R_{\mu fr}$ value is reduced from the baseline $R_{\mu fr}$ value to adequately adjust the peak floor acceleration demands when using the Section A.10.6 equation. The baseline $R_{\mu fr}$ values are calculated in accordance with Section 13.3.1.2 with the following modifications:

1. R_{fr} and Ω_{0fr} are used in lieu of R and Ω_0
2. The value of Ie is taken as 1.0.
3. The lower limit on $R_{\mu fr}$ of 1.3 in Equation 13.3-6 does not apply.

The recommended Rufr values are determined by checking for compliance with the following two criteria:

1. The ratio of the median peak floor acceleration from analysis averaging across all structural levels to the seismic floor acceleration determined in accordance with Section A.10.7 averaged across all structural levels is computed. The average of this ratio across all archetypes within a performance group shall not exceed 1.0.
2. The ratio of the largest peak floor acceleration from analysis at any level to the largest seismic floor acceleration determined in accordance with Section A.10.7 at any structural level is computed. The average of this ratio across all archetypes within a performance group shall not exceed 1.2.

The Section A.8.3.6 evaluation was completed, resulting in the following $R_{\mu fr}$ requirements:

For reinforced masonry shear-controlled walls:

- $R_{\mu fr}$ = 0.65 is required for FRC A/B/C (based on design using R_{fr} = 2.5 and Δ_{afr} = 0.50%), which is smaller than the baseline value of 1.05.
- $R_{\mu fr}$ = 0.65 is required for FRC D (based on design using R_{fr} = 3.0 and Δ_{afr} = 0. 50%), which is smaller than the baseline value of 1.15.

For reinforced masonry flexure-controlled walls:

- $R_{\mu fr}$ = 0.85 is required for FRC A/B/C (based on design using R_{fr} = 3.5 and Δ_{afr} = 0.50%), which is smaller than the baseline value of 1.24.
- $R_{\mu fr}$ = 0.90 is required for FRC D(based on design using R_{fr} = 4.0 and Δ_{afr} = 0.50%), which is smaller than the baseline value of 1.33.

4. CONCLUSIONS

This report documents the quantification of the functional recovery seismic performance factors for the Reinforced Masonry Shear Wall (RMSW) system in accordance with the proposed Section A.8.3.6 procedures of the 2026 National Earthquake Hazards Reduction Program (NEHRP) Provisions. The recommended functional recovery seismic performance factors for the SRMSW are summarized in Table 12 and Table 13. These include the functional recovery response modification coefficient, R_{fr}, the functional recovery allowable story drift limit, Δ_{afr}., and the functional recovery structural ductility reduction factor, $R_{\mu fr}$, for estimation of peak floor accelerations.

Results from the assessment showed that the functional recovery performance factors for shear-controlled SRMSWs were primarily governed by damage in the masonry shear wall in the mid-rise performance group, with the design requirements governed by the max acceptance criteria. Flexure-controlled SRMSWs were governed by damage in the masonry shear walls in both performance groups, with the design requirements governed by the mean criteria.

In selecting the performance factors, preference was given to performance factor combinations with tighter drift limits and R_{fr} at or near the judgement-based limit. This approach was taken because safety-critical structural damage results from excessive displacement, and enforcing stricter drift limits is the more direct way to control displacements. For shear-controlled SRMSWs, an R_{fr} of 2.5 and 3.0 achieves the performance goals for FRC A/B/C and FRC D, respectively, at the design drift limit Δ_{afr} of 0.5%. For flexure-controlled SRMSWs, an R_{fr} of 3.5 and 4.0 achieves the performance goals for FRC A/B/C and FRC D, respectively, at the design drift limit Δ_{afr} of 0.50%.

Table 12. Summary of functional recovery seismic performance factors for SRMSW flexure-dominated lateral systems.

	FRC A/B/C			FRC D		
	R_{fr}	Δ_{afr}	$R_{\mu fr}$[†]	R_{fr}	Δ_{afr}	$R_{\mu fr}$[†]
Analysis results	3.5	0.5%	0.85	4.0	0.5%	0.90
Judgment-based upper limit	3.5	1.0%	--	4.0	1.0%	--
Recommendation – SRMSW-F	**3.5**	**0.5%**	**0.85**	**4.0**	**0.5%**	**0.90**

[†]$R_{\mu fr}$ is only calculated for the recommended seismic performance factors
[*]*Equivalent to the baseline value calculated using R_{fr}*

Table 13. Summary of functional recovery seismic performance factors for SRMSW shear-dominated lateral systems.

	FRC A/B/C			FRC D		
	R_{fr}	Δ_{afr}	$R_{\mu fr}$[†]	R_{fr}	Δ_{afr}	$R_{\mu fr}$[†]
Analysis results	2.5	0.5%	0.65	3.0	0.5%	0.70
Judgment-based upper limit	3.5	1.0%	--	4.0	1.0%	--
Recommendation – SRMSW-S	**2.5**	**0.5%**	**0.65**	**3.0**	**0.5%**	**0.65**

[†]$R_{\mu fr}$ is only calculated for the recommended seismic performance factors
[*]*Equivalent to the baseline value calculated using R_{fr}*

SUPPLEMENTARY MATERIAL

Two supplementary files are attached to this Prequalification Report that provide additional detailed information on the structural response and ATC-138 outcomes from individual archetype models and performance groups, as well as performance outcomes from the independent-strength-and-stiffness check discussed in the body of the report. A general description of the content in each file is provided below to assist with navigation and comprehension of the detailed results.

- **Analysis Report Tables**
  (*"SupplementalData_AnalysisReportTables_RMSW_v3_5_final.xls"*)
  - Contains detailed analysis outcomes for each archetype model assessed, including results for FRC A/B/C and FRC D.
  - "Summary" tab provides a summary of the controlling design values and other response metrics for each archetype.
  - "All Runs" tab provides response and performance outcomes for all combinations of model runs for each archetype.
- **Archetype Performance Plots**
  (*"SupplementalData_ArchtypePerformancePlotsAppendix_RMSW_v3_5_final.pdf"*)
  - Provides visualizations of analysis outcomes similar to the figures in the report, but for the independent-strength-and-stiffness check.
  - Provides visualizations of analysis outcomes similar to the figures in the report, but for individual archetype models.
  - Provide peak transient drift, residual drift, and peak floor acceleration response profiles for each archetype model.

REFERENCES

Ahmadi Koutalan, F. (2012). "Displacement-based Seismic Design and Tools for Reinforced Masonry Shear-Wall Structures," *PhD Dissertation*, University of Texas at Austin.

Almeter, E., Wade, K.F., Haselton, C.B., Saxey, B. (2018). "Rapid Risk Assessment of Buckling Restrained Braced Frames, With Focus on Residual Drifts," *Proceedings of the 11th U.S. National Conference on Earthquake Engineering* (11NCEE), Los Angeles, CA.

Almeter, E., DeBock, D.J., Haselton, C.B. (2024). *Structural Response Prediction Method for SpeedCore Buildings*, Prepared by Haselton Baker Risk Group for the American Institute for Steel Construction, Chicago, IL.

ASCE. (2022). "Minimum Design Loads and Associated Criteria for Buildings and Other Structures," *ASCE/SEI 7-22*, American Society of Civil Engineers, Reston, VA.

ASCE. (2023). "Seismic Evaluation and Retrofit of Existing Buildings," *ASCE/SEI 41-23*, American Society of Civil Engineers, Reston, VA.

ATC. (2021). "Seismic Performance Assessment of Buildings: Volume 8 – Methodology for Assessment of Functional Recovery Time, *ATC-138-3*, Preliminary report for FEMA P-58-8, Prepared by the Applied Technology Council for the Federal Emergency Management Agency, Washington, DC.

Atkinson, R.H., Kingsley, G.R. (1985). "A Comparison of the Behavior of Clay and Concrete Masonry in Compression," *Report No. 1.1-1*, US-Japan Coordinated Program for Masonry Building Research, Atkinson-Noland & Associates, Boulder, CO.

Bažant, Z.P., Oh, B.H. (1983). "Crack band theory for fracture of concrete," *Materials and Structures*, **16**: 155-177.

Blowes, K., Molina Hutt, C., Zimmerman, R., Cook, D.T., Almeter, E., Haselton, C.B. (in press). "Limiting Safety-Critical Structural Damage in Recovery-Based Seismic Design Provisions," *Earthquake Spectra*.

Charney, F. A. (2008). "Unintended Consequences of Modeling Damping in Structures," *Journal of Structural Engineering*, **134**(4): 581-592.

Cheng, J., Shing, P.B. (2018). "Proposed Update of Nonlinear Models for Reinforced Masonry Shear Walls in ASCE 41," *Proceedings of the 11th U.S. National Conference on Earthquake Engineering*, Los Angeles California.

Cheng, J. (2021). "Seismic Performance Evaluation of Reinforced Masonry Wall Systems with Frame Modeling," *PhD Dissertation*, University of California, San Diego.

Cheng, J., Shing, P.B. (2022). "Practical Nonlinear Analysis Methods for Flexure-Dominated Reinforced Masonry Shear Walls," *Journal of Structural Engineering*, **148**(8): 04022109.

Cheng, J., Shing, P.B. (2022b). “A beam-column element for modeling nonlinear flexural and shear behaviors of reinforced masonry,” *Earthquake Engineering and Structural Dynamics*, **51**(8): 1918-1942.

Chopra, A. K., McKenna, F. (2016). “Modeling viscous damping in nonlinear response history analysis of buildings for earthquake excitation,” *Earthquake Engineering and Structural Dynamics*, **45**:193-211.

Coleman, J., Spacone, E. (2001). “Localization issues in force-based frame elements,” *Journal of Structural Engineering*, **127**(11): 1257-1265.

Cook, D., Wade, K., Haselton, C., Baker, J. W., & DeBock, D. J. (2018). A structural response prediction engine to support advanced seismic risk assessment. In *Eleventh US national conference on earthquake engineering, Los Angeles, CA*.

DeBock, D., Manousakis, I.V., Deierlein, G.G., Zsarnóczay, A. (2024). “Updated Model and Criteria for Residual Drift,” *FEMA P-58/BD-3.7.26*, Background documentation for the ATC-138/FEMA P-58 Project, Submitted to the Applied Technology Council, Prepared for the Federal Emergency Management Agency, Washington, DC.

Deierlein, G.G., Victorsson, L. (2008). *Fragility Curves for Steel Beam-Column Connections in FEMA P-58*, Prepared for the Federal Emergency Management Agency, Washington, DC.

FEMA. (2009a). “Quantification of Building Seismic Performance Factors,” *FEMA P695*, Prepared by the Applied Technology Council for the Federal Emergency Management Agency, Washington, DC.

FEMA. (2009b). “Damage States and Fragility Curves for Reinforced Masonry Shear Walls,” *FEMA P-58/BD-3.8.10*, Prepared by the Applied Technology Council for the Federal Emergency Management Agency, Washington, DC.

FEMA. (2018). “Seismic Performance Assessment of Buildings: Volume 1 - Methodology,” *FEMA P-58-1*, 2nd Edition, Prepared by Juan Murcia-Delso, P. Benson Shing and the Applied Technology Council for the Federal Emergency Management Agency, Washington, DC.

FEMA. (2018b). “Seismic Performance Assessment of Buildings: Volume 2 – Implementation Guide,” *FEMA P-58-2*, 2nd Edition, Prepared by the Applied Technology Council for the Federal Emergency Management Agency, Washington, DC.

FEMA. (2020). “Short-Period Building Collapse Performance and Recommendations for Improving Seismic Design: Volume 3 – Study of One-to-Four Story Special Reinforced Masonry Shear Wall Buildings,” *FEMA P-2139-3*, Prepared by the Applied Technology Council for the Federal Emergency Management Agency, Washington, DC.

Fitzgerald, K., Haselton, C., Baker, J., Cook, D. (2016). "Fragility Functions for the Precast Hybrid Moment Frame System," Prepared by Haselton Baker Risk Group for Clark Pacific, West Sacramento, CA.

Hall, J. (2006). "Problems encountered from the use (or misuse) of Rayleigh damping," *Earthquake Engineering and Structural Dynamics*, **35**: 525-545.

Haselton Baker Risk Group (2025). Seismic Performance Prediction Program (SP3).

Jansen, D.C., Shah, S.P. (1997). "Effect of length on compressive strain softening of concrete," *Journal of Engineering Mechanics*, **123**(1): 25-35.

Kapoi, C.M. (2012). "Experimental Performance of Concrete Masonry Shear Walls Under In-Plane Loading," *MSc Thesis*, Washington State University, Pullman, WA.

Kent. D.C., Park, R. (1974). "Flexural members with confined concrete," *Journal of the Structural Division*, **97**(7): 1969-1990.

Kingsley, G.R., Shing, P.B., Gangel, T. (2014). "Seismic Design of Special Reinforced Masonry Walls," *NIST GCR 14-917-31*, National Institute of Standards and Technology, Gaithersburg, MD.

Kolozvari, K., Orakcal, K., Wallace J.W. (2015). "Shear-Flexure Interaction Modeling of reinforced Concrete Structural Walls and Columns under Reversed Cyclic Loading," *PEER Report No. 2015/12*, Pacific Earthquake Engineering Research Center, University of California, Berkeley.

Koutras, A. (2019). "Assessment of the Seismic Behavior of Fully and Partially Grouted Reinforced Masonry Structural Systems Through Finite Element Analysis and Shake-table Testing," *PhD Dissertation*, University of California, San Diego.

Lepage, A., Sanchez, R.E. (2012). "Practical Nonlinear Analysis for Limit Design of Reinforced Masonry Walls," *The Open Civil Engineering Journal*, **6**: 107-118.

Liu, J., Astaneh-Asl, A. (2000). *Cyclic Testing of Simple Steel Shear Tab Connections*, Report No. UCB/CEE-Steel-2000/01, University of California, Berkeley, CA.

Mavros, M. (2015). "Experimental and Numerical Investigation of the Seismic Performance of Reinforced Masonry Structures," *PhD Dissertation*, University of California, San Diego.

Miranda, E. (1999). "Approximate seismic lateral deformation demands in multistory buildings," *Journal of Structural Engineering*, **125**(4): 417-425.

Miranda, E., Reyes, C.J. (2002). "Approximate lateral drift demands in multistory buildings with nonuniform stiffness," *Journal of Structural Engineering*, **128**(7): 840-849.

McKenna, F., Scott, M.H., Fenves, G.L. (2010). "Nonlinear Finite-Element Analysis Software Architecture using Object Composition," *Journal of Computing in Civil Engineering*, **24**(1): 95-107.

Murcia-Delso, J. and Shing, P. B. (2012). "Fragility Analysis of Reinforced Masonry Shear Walls," *Earthquake Spectra*, Volume 20, No. 4, pages 1523-1527, November 2012.

NIST. (2010). "Evaluation of the FEMA P-695 Methodology for Quantification of Building Seismic Performance Factors," *NIST GCR 10-917-8*, Prepared by the NEHRP Consultants Joint Venture (ATC and CUREE) for the National Institute of Standards and Technology, Gaithersburg, MD.

NIST. (2017). "Recommended Modeling Parameters and Acceptance Criteria for Nonlinear Analysis in Support of Seismic Evaluation, Retrofit, and Design," *NIST GCR 17-917-45*, Prepared by the Applied Technology Council for the National Institute of Standards and Technology, Gaithersburg, MD.

Orakcal K., Conte J.P., Wallace J.W. (2004). "Flexural Modeling of Reinforced Concrete Structural Walls - Model Attributes," *ACI Structural Journal*, **101**(5): 688-698.

Shedid, M.T., Drysdale, R.G., El-Dakhakhni, W.W. (2008). "Behavior of fully grouted reinforced concrete masonry shear walls failing in flexure: experimental results," *Journal of Structural Engineering*, **134**(11): 1754-1767.

Sherman, J.D. (2011). "Effects of Key Parameters on the Performance of Concrete Masonry Shear Walls Under In-Plane Loading," *MSc Thesis*, Washington State University, Pullman, WA.

Shing, P.B., Noland, J.L., Spaeh, H.P., Klamerus, E.W., and Schuller, M.P. (1991), "Response of Single-Story Reinforced Masonry Shear Walls to In-Plane Lateral Loads." *Report No. 3.1(a)-2*, US-Japan Coordinated Program for Masonry Building Research, University of Colorado at Boulder, Boulder, CO.

Terzic, V., Kolozvari, K. (2020). "Evaluation of Post-Earthquake Functional Recovery for a 42-Story Building Located in Los Angeles," *Proceedings of 2020 Los Angeles Tall Buildings Structural Design Council Annual Conference*.

TMS. (2016). "Building Code Requirements and Specifications for Masonry Structures," *TMS 402/602*, The Masonry Society, Boulder, CO.

Vamvatsikos, D., Cornell, C.A. (2002). "Incremental Dynamic Analysis," *Earthquake Engineering and Structural Dynamics*, **31**(3): 491-514.

Vulcano A., Bertero V.V., Colotti V. (1988). "Analytical Modeling of RC Structural Walls," *Proceedings, 9th World Conference on Earthquake Engineering*, V. 6, Tokyo-Kyoto, Japan, pp. 41-46.